2021년 2월
석사학위논문

Pathophysiological analysis of articular cartilage degeneration through 7α,25-Dihydroxycholesterol-induced oxiapoptophagy

조선대학교 대학원

치의생명공학과

김 태 현

Pathophysiological analysis of articular cartilage degeneration through 7α,25-Dihydroxycholesterol-induced oxiapoptophagy

7α,25-Dihydroxycholesterol의 자가포식
세포사멸 유도에 의한 병태생리학적 연골퇴행성 분석

2021년 2월 25일

조선대학교 대학원

치의생명공학과

김 태 현

Pathophysiological analysis of articular cartilage degeneration through 7α,25-Dihydroxycholesterol-induced oxiapoptophagy

지도교수 김 재 성

이 논문을 치의생명공학 석사학위신청 논문으로 제출함.

2020년 10월

조선대학교 대학원

치의생명공학과

김 태 현

김태현의 석사학위논문을 인준함

위원장 조선대학교 교 수 김 흥 중 (인)

위 원 조선대학교 교 수 김 도 경 (인)

위 원 조선대학교 교 수 김 재 성 (인)

2020 년 11 월

조선대학교 대학원

TABLE OF CONTENT

LIST OF TABLES

LIST OF FIGURES

LIST OF ABBREVIATIONS

25-HC ····· 25-hydroxycholesterol
7α,25-DHC ····· 7α,25-dihydroxycholesterol
ADAMTS ····· A disintegrin and metalloproteinase with thrombospondin motifs
Annexin V-FITC ····· Annexin V-fluorescein isothiocyanate
Bad ····· Bcl-2-associated death promoter
Bax ····· Bcl-2-associated X protein
Bcl-2 ····· B-cell lymphoma 2
Bcl-xL ····· B-cell lymphoma extra-large
Bid ····· Bax-like BH3 protein
BSA ····· Bovine serum albumin
CH25H ····· Cholesterol-25-hydroxylase
Col II ····· Type II collagen
COX-2 ····· Cyclooxygenase-2
CYP7B1 ····· Cholesterol by cytochrome P450 family 7 subfamily B member 1
DAPI ····· 4’,6-Diamidino-2-phenylindole dihydrochloride
DMEM/F-12 ····· Dulbecco’s modified eagls’s medium/nutrient mixture F-12
DMM ····· Destabilization of median meniscus
DMSO ····· Dimethyl sulfoxide
ECM ····· Extracellular matrix
EDTA ····· Ethylenediaminetetraacetic acid
FACS ····· Fluorescence activated cell sorter
FasL ····· Fas ligand
FBS ····· Fetal bovine serum
GAPDH ····· Glyceraldehyde 3-phosphate dehydrogenase
H&E ····· Hematoxylin & eosin
IACUC ····· Institutional Animal Care and Use Committee
IHC ····· Immunohistochemistry
IL-1β ····· Interleukin-1β

IL-6 ····· Interleukin-6
iNOS ····· Inducible nitric oxide synthase
LC3 ····· Microtubule-associated proteins 1A/1B light chain 3B
LPS ····· Lipopolysaccharides
PVDF ····· Polyvinylidene fluoride
MBLI ····· MBL international
MMPs ····· Matrix metalloproteinase
MTT ····· Dimethyl thiazolyl diphenyl tetrazolium salt
NO ····· Nitric oxide
OA ····· Osteoarthritis
PARP ····· Poly ADP-ribose polymerase
PBS ····· Phosphate buffered saline
PCR ····· Polymerase chain reaction
PGE_2 ····· Prostaglandin E_2
PI ····· Propidium iodide
PTGS2 ····· Post-transcriptional gene silencing 2
PVDF ····· Polyvinylidene fluoride
qPCR ····· Quantitative polymerase chain reaction
qRT-PCR ····· Quantitative real-time PCR
RA ····· Rheumatoid arthritis
RORα ····· Retinoic acid-related orphan receptor α
RT ····· Room temperature
tBID ····· Truncated Bid
TBS-T ····· Tris buffered saline with Tween 20
TIMPs ····· Tissue inhibitors of metalloproteinases
TNF-α ····· Tumor necrosis factor-α

ABSTRACT

Pathophysiological analysis of articular cartilage degeneration through 7α,25-Dihydroxycholesterol-induced oxiapoptophagy

Kim Tae-Hyeon
Advisor : Prof. Kim Jae-Sung, Ph.D.
Department of Dentistry
Biodental Engineering of Chosun University

The aim of the present study was to investigate the pathophysiology of articular cartilage degeneration induced by oxiapoptophagy, a type of cell death accompanied by oxysterol-induced apoptosis and autophagy, in chondrocytes and articular cartilages treated with 7α,25-dihydroxycholesterol (7α,25-DHC). Lipopolysaccharide (LPS)-induced inflammation increased cell death and upregulated CYP7B1 expression in primary rat chondrocytes, which indicates that LPS-induced cell death involves the 7α,25-DHC synthesized by upregulated CYP7B1. The present study showed that 7α,25-DHC not only accelerated proteoglycan loss from articular cartilage, but also decreased the mRNA induction of type II collagen and aggrecan, major components of articular cartilage, in chondrocytes. Furthermore, 7α,25-DHC upregulated the expression and activity of cartilage-degrading enzymes, such as matrix metalloproteinase (MMP)-13 and MMP-1, and increased the levels of inflammatory mediators, such as inducible nitric oxide synthase (NO), cyclooxygenase-2 (COX-2), nitric oxide, and prostaglandin E_2 (PGE_2) in chondrocytes. Moreover, 7α,25-DHC not only increased cytotoxicity in primary rat chondrocytes, but also increased the number of chondrocytes with condensed chromatin in a dose-dependent manner. Moreover, 7α,25-DHC-induced cell death was mediated by extrinsic and intrinsic apoptosis in chondrocytes in a

caspase-dependent manner. In addition, biomarkers of autophagy, such as beclin-1 and microtubule-associated protein 1A/1B-light chain 3, increased in chondrocytes treated with 7α,25-DHC. Finally, the immunoreactivity of CYP7B1, caspase-3, and beclin-1 increased in the articular cartilage that exhibited severe proteoglycan loss due to destabilization of the median meniscus in the knee joints of mice. Taken together, our data indicate that 7α,25-DHC induces progressive articular degeneration via accelerating proteoglycan loss caused by the upregulation of catabolic factors, such as cartilage-degrading enzymes and inflammatory mediators, as well as the oxiapoptophagy of chondrocytes through caspase-dependent extrinsic and intrinsic apoptosis accompanied by autophagy. Furthermore, these data suggest that metabolic syndrome may be a critical risk factor for the induction of osteoarthritis by upregulating pathophysiological oxysterols, including 7α,25-DHC, synthesized through cholesterol oxidation.

I. INTRODUCTION

A joint (articulation) is a functional point that connects the skeletal system by forming junctions between the ends of bones. In particular, synovial joints, called diarthroses, are considered the main functional joints of the body and are freely moveable via abduction, adduction, extension, flexion, and rotation, which result from the contraction or relaxation of the muscles that are attached to the bones on either side of the articulation [1].

To allow the primary mechanical function of the synovial joint, the synovial cavity, surrounded by the articular capsules (fibrous connective tissues attached to each end of the participating bones), is filled with synovial fluid, secreted by the synovial membrane, and covers the articulating surfaces composed of articular cartilage at the end of each bone. Articular cartilage, which is avascular, anural, and alymphatic, is hyaline cartilage composed of dense extracellular matrix (ECM) [2]. Generally, articular cartilage is composed mainly of type II collagen (Col II), proteoglycan, non-collagenous proteins, and glycoproteins; this allows articular cartilage to retain water, which plays an important role in maintaining typical mechanical properties such as shock absorption and friction reduction during body movement [3]. Furthermore, these components are maintained by highly specialized cells called chondrocytes, which are distributed sparsely in dense ECM. Chondrocytes differentiate from mesenchymal stem cells during the developmental process and are constitute approximately 1-5% of the total articular cartilage tissue [4]. Hence, the malfunction of synovial joints caused by the progressive breakdown of articular cartilage and apoptosis of chondrocytes could restrict body movements [5].

The homeostasis of articular cartilage is regulated by anabolism (synthesis) and catabolism (degradation) in the microenvironment of synovial joints. In a normal cartilage, anabolism and catabolism are well equilibrated through finely balanced anabolic and catabolic gene expression [6]. Generally, anabolic factors, such as transforming growth factor-β, insulin-like growth factor-1, and bone morphogenetic

protein-7, increase the synthesis of ECM components, such as proteoglycan and Col II, by stimulating chondrocytes [7]. Catabolic factors such as pro-inflammatory cytokines, including interleukin-1β (IL-1β), interleukin-6 (IL-6), and tumor necrosis factor-α (TNF- α), inflammatory mediators, including inducible nitric oxide (iNOS), cyclooxygenase-2 (COX-2), prostaglandin E_2 (PGE_2), and nitric oxide (NO), and catabolic growth factors induce the progressive breakdown of articular cartilage via elevated expression and activity of cartilage-degrading enzymes, such as matrix metalloproteinase (MMPs) and a disintegrin and metalloproteinase with thrombospondin motifs (ADAMTS) as well as suppress tissue inhibitors of metalloproteinases (TIMPs) in chondrocytes [8]. Further progressive degeneration of articular cartilage reduces the space in the synovial joint through the disruption of articular cartilage integrity and apoptosis of chondrocytes. Sequentially, reduced space of the synovial joint induces chronic and severe joint pain, which limits joint mobility [9].

Osteoarthritis (OA) is a chronic joint disease that can affect multiple joints; it causes severe joint pain due to the degeneration of articular cartilage in synovial joints [10]. Generally, the symptoms of arthritis express over time in adults over the age of 65, but it may also suddenly appear in children, teenagers, and younger adults. Although the pathophysiological etiology of arthritis remains largely unknown, recent studies have shown that arthritis is closely associated with chronic oxidative stress and inflammation in synovial joints [11]. The etiology of arthritis is multifactorial, including aging, obesity, joint malalignment, traumatic joint injury, and genetic predisposition, and involves the disruption of homeostasis via an increased catabolism, and decreased anabolism in the synovial joint [12]. The imbalance between anabolism and catabolism due to these risk factors can lead to chronic oxidative stress and increase the production of pro-inflammatory cytokines and inflammatory mediators that can trigger the degeneration of articular cartilage in synovial joints [13].

OA is a chronic age-related disease accompanied by low-grade chronic systemic inflammation that has recently been called “inflammaging” [14]. Although the

pathophysiological cellular pathways of inflammation remain largely unknown in arthritis, they generally contribute to the impairment of the mechanical function of synovial joints via increasing the release of pro-inflammatory cytokines due to chronic oxidative stress, accelerating degeneration of articular cartilage caused by upregulated articular cartilage-degrading enzymes, and increasing autophagy and apoptosis of chondrocytes [15].

Generally, obesity, defined as an excess of body fat, is a known cause of metabolic diseases, such as coronary artery disease, hypertension, type 2 diabetes mellitus, respiratory disorders, and dyslipidemia, owing to increased fasting plasma triglycerides, high low-density lipoprotein cholesterol, low high-density lipoprotein cholesterol, elevated levels of blood glucose and insulin, and high blood pressure [16]. Furthermore, obesity, a pathophysiological risk factor of arthritis, induces the progressive degeneration of articular cartilage via the structural damage to the joint resulting from increased mechanical overload on the synovial joints and the generation of low-grade inflammation due to the aberrant expression of adipokines. Therefore, recent studies have suggested arthritis as a metabolic disease accompanied with inflammation [17].

Cholesterol is an amphiphilic hydrocarbon compound containing four hydrocarbon steroid rings between the partly hydrophilic hydroxyl group and the hydrophobic hydrocarbon chain [18]. A cholesterol acts as a precursor of steroid hormones, vitamin D, and bile acid to maintain physiological homeostasis including sterol metabolism and cellular signaling associated with cell growth, proliferation, and migration. In addition, cholesterol is an essential structural molecule that maintains the stability of animal cell membranes by modulating membrane fluidity [19].

Oxysterols are oxidized forms of cholesterol generated from cholesterol by auto-oxidation, enzymatic processes, or both. Some oxysterols induce oxiapoptophagy, a type of cell death associated with oxidative stress that has several characteristics of apoptosis and autophagy [20]. Oxidative stress is associated with the overproduction

of reactive oxygen species, increased antioxidant enzyme activities, lipid peroxidation, and protein carbonylation. Apoptosis is associated with activation of the mitochondrial pathway, opening of the mitochondrial permeability pore, loss of mitochondrial membrane potential, caspase-3 activation, poly ADP-ribose polymerase (PARP) degradation, nuclear condensation, and fragmentation. Autophagy is characterized by microtubule-associated proteins 1A/1B light chain 3B (LC3) and Beclin-1 [21].

Recent studies have reported that 25-hydroxycholesterol (25-HC), an oxysterol synthesized from cholesterol by cholesterol-25-hydroxylase (CH25H), not only induces apoptotic cell death in various types of cells, such as the motor neuron-like cell line NSC34 and head and neck squamous cell carcinoma cells FaDu, but also induces P2X7-dependent pyroptosis in human keratinocytes [22-24]. A recent study reported that the CH25H-CYP7B1 (cholesterol by cytochrome P450 family 7 subfamily B member 1)-retinoic acid-related orphan receptor α (RORα) axis is involved in OA and that 25-HC acts as a pathophysiological oxysterol of OA to induce apoptotic cell death in chondrocytes [25].

As shown in Figure 1, 7α,25-dihydroxycholesterol (7α,25-DHC) is an oxysterol synthesized from CYP7B1 (also known as 25-hydroxycholesterol 7α-hydroxylase) under inflammatory conditions. Based on these studies, it was hypothesized that 7 α,25-DHC, a downstream oxysterol of 25-HC, may act as a pathophysiological oxysterol to induce OA by increasing apoptosis in the chondrocytes in a manner similar to that of 25-HC. Hence, the aim of the present study was to investigate the pathophysiological role of 7α,25-DHC as a metabolic risk factor of OA to provide a biological link between metabolic syndrome and OA.

II. MATERIALS AND METHODS

II-1. Chemicals and antibodies

7α,25-DHC was purchased from Tocris Cookson Ltd (Minneapolis, MN, USA) and was dissolved in ethanol at stock concentration (10 mg/mL). Antibodies for FasL (sc-19988, 48 kDa), caspase-3 (CST#9662, 17 and 34 kDa), caspase-8 (CST#4790, 25 and 53 kDa), caspase-9 (CST#9508, 35 and 47 kDa), PARP (CST#9542, 116 kDa), β -actin (CST#4970, 42 kDa), Bcl-2 (sc-7382, 26 kDa), Bcl-xL (sc-8392, 26 kDa), Bax (CST#2772, 21 kDa), Bid (sc-56025, 22 and 15 kDa), Bad (CST#9292, 23 kDa), iNOS (CST#13120, 130 kDa), Beclin-1 (sc-48341, 60 kDa), MMP-13 (sc-101564, 48 kDa), MMP-3 (sc-21732, 57 kDa), COX-2 (sc-376861, 60 kDa), CYP7B1 (bs-50852R, 48 kDa), CH25H (sc-293256, 32 and 26 kDa) and secondary antibodies were purchased from Santa Cruz Biotechnology Inc. (Dallas, TX, USA). LC3 (16 and 18 kDa) was purchased from MBL international (Woburn, MA, US).

II-2. Isolation and culture of primary rat chondrocyes

Primary rat chondrocytes were isolated from the articular cartilage of rat (5-day-old; Sprague-Dawely rats) knee joins, in accordance with the protocol approved by the Institutional Animal Care and Use Committee of Chosun University, Gwangju, Republic of Korea (CIACUC2020-A0011). Isolated primary rat chondrocytes were maintained in Dulbecco's Modified Eagls's Medium/Nutrient Mixture F-12 (DMEM/F-12) (Thermo Scientific, Rockford, IL, USA) supplemented with 10% fetal bovine serum (FBS), antibiotics (50 U/mL penicillin and 50 μg/mL streptomycin), and 50 μg/mL ascorbic acid.

II-3. Quantitative polymerase chain reaction (qPCR) and quantitative real-time PCR (qRT-PCR)

Chondrocytes were treated with either lipoplysaccharide (LPS) or 7α,25-DHC for 48 h. Thereafter, total RNA was isolated from the chondrocytes using TRIzol reagent (Invitrogen, CA, USA) according to the manufacturer's instructions. The concentration of the isolated total RNA was measured using a Nanodrop 2000 (ThermoFisher Scientific, MA, USA). To synthesize cDNA, 1 μg RNA was reverse transcribed using a ThermoScript reverse transcribtion-PCR system (IInvitrogen, California, USA) according to the manufacturer's instructions. For qRT-PCR, cDNA was amplified using an Eco Real-Time PCR system (illumine Inc, San Diego, CA, USA). Relative gene expression was determined using the $^{\Delta\Delta}$CT method, as detailed by the manufacturer (illumine Inc, San Diego, CA, USA). qPCR was performed using 2 x TOPsimple DyeMIX-*n*Taq (Enzynomics, Seoul, Korea) and specific primers on a TaKaRa PCR Thermal Cycler Dice (TaKaRa Bio Inc., Shiga, Japan). Thereafter, the PCR products were electrophoresed on an agarose gel to determine the expression level of the target genes. Glyceraldehyde 3-phosphate dehydrogenase (GAPDH) was used as an internal control. The primer sequences and the conditions used are summarized in Table 1 and Table 2.

II-4. Western blotting

Chondrocytes were cultured in a 6-well plate and treated with either LPS or 7 α,25-DHC for 48 h. Thereafter, total proteins were extracted from the chondrocytes using a cell lysis buffer (Cell Signaling Technology, MA, USA), according to the manufacturer's instructions. The protein concentration was determined using a bicinchoninic acid protein assay (ThermoFisher Scientific, MA, USA). Equal amounts of each protein sample were electrophoresed on 10% sodium dodecyl sulfate polyacrylamide gel and subsequently transferred to polyvinylidene fluoride (PVDF) membrane (Millipore, Burlington, MA, USA) at 4°C. Thereafter, the PVDF membrane was blocked using 5% (v/v) bovine serum albumin (BSA; Sigma-Aldrich, ST. Louis, MO, USA) prepared in

Tris buffered saline with Tween 20 (TBS-T) (Santa Cruz Biotechnology Inc., Dallas, TX, USA) and then incubated with the primary antibodies at 4℃. The following primary antibodies purchased from Santa Cruz Biotechnology Inc. and diluted 1:1,000 in TBS-T containing 5% (v/v) BSA were used: antibodies against FasL, Bcl-2, Bcl-xL, and Bid. In addition, the following primary antibodies purchased from Cell Signaling Technology and diluted 1:1,000 in TBS-T containing 5% (v/v) BSA were also used: antibodies against caspase-8, caspase-3, PARP, Bad, Bax, caspase-9, and β-actin. The immunoreactive bands were visualized using the ECL System (Amersham Biosciences, Piscataway, NJ, USA), exposed on radiographic film or MicorChemi 4.2 (Dong-Il Shimadzu Corp., Seoul, Korea).

II-5. *Ex vivo* organ culture of rat articular cartilage tissues

Articular cartilage tissues were isolated from the knee joints of 5-day-old Sprague-Dawley rats and then cultured in DMEM/F12 supplemented with 10% FBS. Next, the articular samples were treated with 0, 25 and 50 μg/mL 7α,25-DHC for 14 days. At the end of the culture period, the samples were collected and fixed in 4% paraformaldehyde for 72 h to perform histological analysis.

II-6. Histological analysis

Histological analysis using safranin-O and fast green staining was performed to verify proteoglycan loss in the articular cartilage treated with 0, 25 and 50 μg/mL 7α,25-DHC for 14 days. Briefly, fixed articular cartilage samples were decalcified in ethylenediaminetetraacetic acid (EDTA) and then embedded in paraffin. Thereafter, the prepared paraffin blocks containing articular cartilage were serially sliced to 7-8 μm thickness and placed on slides. Safranin-O and fast green staining was subsequently performed to assess proteoglycan loss in the articular cartilage ground substance. In addition, hematoxylin and eosin (H&E) staining was performed to observe the general morphology of the articular cartilage.

II-7. Gelatin zymography

Gelatin zymography was performed to assess the activation of MMPs in primary rat chondrocytes. Briefly, primary rat chondrocytes were treated with 25 and 50 μg/mL 7 α,25-DHC for 48 h. Thereafter, an equal volume of conditioned medium was electrophoresed on a 10% polyacrylamide gel containing copolymerized 0.2% (1 mg/mL) porcine skin gelatin. After electrophoresis, the gel was incubated in zymogram renaturing buffer (50 mM Tris-HCI (pH 7.6), 10 mM $CaCl_2$, 50 mM NaCl, and 0.05% Brij-35) at 37°C for 72 h. After renaturation of MMPs, the gel was stained with 0.1% Coomassie Brilliant Blue R250. Gelatinolytic bands were revealed as clear bands on a background uniformLy stained light blue and then imaged using a digital camera.

II-8. Measurement PGE_2 production

Primary chondrocytes were seed at 1×10^6 cells/mL in a 6 well culture plate. Chondrocytes were treated with 0, 25, and 50 μg/mL 7α,25-DHC for 48 h. The production of PGE_2 was measured using a Parameter™ PGE_2 assay kit (ThermoFisher Scientific, MA, USA), according to manufacturer's protocol.

II-9. Measurement of NO

Primary rat chondrocytes were treated with 0, 25, and 50 μg/mL 7α,25-DHC for 48 h. Thereafter, 100 μL of the conditioned medium was reacted with 100 μL each of sulfanilamide and N-1-naphthylethylenediamine dihydrochloride. Absorbance was then measured at 540 nm wavelength using a spectrophotometer (Epoch Spectrophotometer, Bio Tek, Winooski, VT, USA).

II-10. Cell viability assay

Chondrocytes (1×10^6 cells/mL) were cultured in 96-well culture plates, and then treated with either LPS or 7α,25-DHC for 24 and 48 h. Following addition of the dimethyl thiazolyl diphenyl tetrazolium salt (MTT) solution, the chondrocytes were further cultured for 4 h. After incubation, the MTT crystals that formed were suspended completely in dimethyl sulfoxide (DMSO; Sigma-Aldrich, St. Louis, MO, USA) and the absorbance was read at 570 nm using a spectrometer (Epoch microplate spectrophotometer; BioTek, Winooski, VT, USA).

II-11. H&E staining

Chondrocytes (1×10^6 cells/mL) were cultured in an 8-well chamber slide (Sigma-Aldrich, ST. USA) and treated with 0, 1, 10, 25 and 50 μg/mL of 7α,25-DHC for 48 h at 37°C. Subsequently, chondrocytes were fixed with 4% paraformaldehyde for 30 min at room temperature (RT). H&E staining was performed to evaluate the morphological alterations in chondrocytes. Cells were observed and imaged using Leica DM750 microscope (Leica Microsystems, Heerbrugg, Switzerland).

II-12. Cell survival assay

Cell survival assay was performed to assess the survival of chondrocytes treated with either LPS or 7α,25-DHC using a Live/Dead assay kit (Molecular Probes, Carlsbad, CA, USA), which consists of green calcein AM for labeling live cells and ethidium homodimer-1 for labeling dead cells. Chondrocytes were cultured on 8-well chamber slides (Nunc Lab-Tek II Chamber Slide system; Sigma-Aldrich ST, Louis, MO, USA), and then treated with either LPS or 7α,25-DHC for 48 h. After cultivation, cell survival assay was performed according to the manufacturer's instructions. Thereafter, the stained cells were imaged using a fluorescence microscope (Eclipse TE200; Nikon Instruments, Melville, NY, USA) and counted to plot the histogram.

II-13. Nuclear staining

Chondrocytes were cultured on an 8-well chamber slide and were treated with 0, 1, 10, and 25 μg/mL 7α,25-DHC for 48 h at 37°C. Thereafter, the cells were rinsed three times with phosphate buffered saline (PBS; Sigma-Aldrich ST, Louis, MO, USA) at RT. The cells were stained with 4',6-diamidino-2-phenylindole dihydrochloride (DAPI; Sigma-Aldrich, ST. USA). Nuclear condensation was observed and imaged using a fluorescence microscope.

II-14. Fluorescence-activated cell sorting (FACS) analysis

Chondrocytes were cultured in a 60ø plate (SPL Life Science Co. Ltd., Pocheon, Korea), then cells were treated with 0, 25 and 50 μg/mL 7α,25-DHC for further 48 h. The chondrocytes were collected, washed with ice-cold PBS, and resuspended in binding buffer (BD Biosciences, San Diego, CA, USA). Thereafter, annexin V-fluorescein isothiocyanate (Annexin V-FITC) and propidium iodide (PI) (Cell Signaling Technology, Danvers, MA, USA) were added to the chondrocytes and incubated for 15 min at 37°C. Changes in the apoptotic populations were analyzed using a BD Cell Quest version 3.3 (Becton Dickinson, San Jose, CA, USA).

II-15. Immunohistochemistry (IHC)

Immunohistochemistry was performed using Vectastain® ABC Kit (Vector Laboratories, Burlingame, CA, USA) tumor masses were excised, post-fixed in 4% paraformaldehyde for 7 days, dehydrated in a series of ethanol solutions (70, 80, 90, and 100%; 2 h per step), and then submerged in xylene twice for 2 h and in paraffin twice for 2 h. Paraffin-embedded tissue blocks were prepared and cut using a microtome. The 8-μ m-thick sections placed on glass slides. The sections were deparaffinized using two changes of xylene for 3 min, rehydrated with two washes each of 100, 90, 80, and 70%

ethanol for 3 min, and then rinsed with tap water for 3 min. The sections incubated at 4°C with caspase-3 antibody overnight and incubated for 1 h at room temperature with peroxidase-conjugated goat anti-mouse antibody. Sections were subsequently counterstained using hematoxylin, transferred to the mounting reagent, and examined by microscopy.

II-16. Caspase-3/-7 activity assay

Chondrocytes were cultured on 8-well chamber slides, and then treated with 0, 1, 10, 25, and 50 μg/mL of 7α,25-DHC for 48 h. Thereafter, the activity of caspase-3/7 was assessed using the cell permeable fluorogenic substrate PhiPhiLux-G_1D_2 (OncoImmunin Inc.; Gaithersburg, MD, USA), according to the manufacturer's instructions, and imaged using fluorescence microscopy.

II-17. Generation of osteoarthritic animals

OA animals were generated by the surgical destabilization of median meniscus (DMM) at knee joint of mouse. Knee joints were dissected respectively at the 3 weeks as a middle stage of OA and 8 weeks as a late stage of OA, after DMM surgery. Thereafter, histological analysis using safranin-O & fast green staining for the proteoglycan of articular cartilage and immunohistochemistry using CYP7B1, caspase-3 and beclin-1 antibodies were performed to investigate the pathophysiological linkages between proteoglycan loss, 7α,25-DHC, apoptosis and autophagy.

II-18. Statistical analysis

Analysis of variance (ANOVA) was performed using the Stat-View 5.0 software (SAS Institute, Cary, NC, USA). p-values < 0.05 were considered statistically significant.

III. RESULTS

III-1. LPS-induced inflammation increases catabolic effects and induces the expression of oxysterol synthase in primary rat chondrocytes

To determine which oxysterol is synthesized in chondrocytes under inflammatory conditions, primary rat chondrocytes were cultured with 2.5 and 5 μg/mL of LPS for 48 h. As shown in Fig. 2, LPS generally induced catabolic effects in chondrocytes. The mRNA levels of major components of articular cartilage, such as Col II and aggrecan, were significantly decreased in the chondrocytes treated with LPS, as shown in Fig. 2A. LPS upregulated the mRNA and protein levels of cartilage-degrading enzymes such as MMP-3 and MMP-13 in chondrocytes, as shown in Fig. 2B and 2C. Furthermore, the mRNA and protein levels of inflammatory mediators, such as iNOS, COX-2, and PTGS2, increased significantly in the chondrocytes treated with LPS, as shown in Fig. 2D and 2E. Moreover, LPS induced apoptotic cell death through the expression of caspase-3 and PARP in chondrocytes, as shown in Fig. 2F. In addition, the level of *ch25h* mRNA, which encodes an *ch25h* enzyme that converts cholesterol to 25-HC, was increased significantly in chondrocytes treated with LPS in a dose-dependent manner, as shown in Fig. 2G. Additionally, the level of *cyp7b1* mRNA, which encodes an *cyp7b1* enzyme that converts 25-HC to 7α,25-DHC, increased in a dose-dependent manner by LPS in chondrocytes. Furthermore, the expression of CH25H and CYP7B1 upregulated in the chondrocytes treated with LPS, as shown in Fig. 2H. Taken together, these data demonstrate that LPS-induced inflammation increases catabolic effects such as the inhibition of the synthesis of articular cartilage components, upregulation of cartilage-degrading enzymes and inflammatory mediators, and increased apoptotic cell death. These findings also suggest that LPS-induced inflammation and apoptotic cell death may involve these oxysterols.

III-2. 7α,25-DHC accelerates proteoglycan loss in articular cartilage

To determine whether 7α,25-DHC acts as a catabolic risk factor to induce the progressive degeneration of articular cartilage, explants of articular cartilage dissected from the knee joint of 5-day-old rats (*ex vivo* organs) were cultured with 10 and 25 μg/mL 7α,25-DHC for 14 days. Thereafter, explants of articular cartilage were fixed with 4% paraformaldehyde for one week and then embedded into paraffin for histological assessment using hematoxylin and eosin (Fig. 3A) to investigate morphological alteration and safranin-O and fast green (Fig. 3B) staining to observe the proteoglycan in articular cartilage. As shown in Fig. 3A, there were no other significant morphological changes in the explants of articular cartilage treated with 7α,25-DHC. However, as shown in Fig. 3B, proteoglycans were depleted from the articular cartilage treated with 10 and 25 μg/mL 7α,25-DHC compared with the untreated controls, in a dose-dependent manner. These data indicate that 7α,25-DHC is a potential catabolic oxysterol that induces the progressive degeneration of articular cartilage through the loss of proteoglycan, a major component of articular cartilage.

III-3. 7α,25-DHC suppress the induction of Col II and aggrecan mRNA in chondrocytes

Next, to verify the 7α,25-DHC-induced catabolic effects on major components of articular cartilage, such as Col II and aggrecan, chondrocytes were cultured with 25 and 50 μg/mL of 7α,25-DHC for 48 h. Thereafter, the changes in Col II and aggrecan mRNA were assessed by qPCR and qRT-PCR, as shown in Fig. 4A and 4B, respectively. The results of qPCR showed that mRNA levels of Col II and aggrecan decreased significantly in chondrocytes treated with 7α,25-DHC, as shown in Fig. 4A. Aggrecan mRNA levels were 14.8 ± 3.6% and 10.6 ± 1.3% in the chondrocytes

treated with 25 and 50 μg/mL 7α,25-DHC for 48 h, respectively, compared with that of the control cells (100.4 ± 9.7%), as shown in Fig. 4B. Col II mRNA levels were 32 ± 3.7% and 25.2 ± 3.5% in the chondrocytes treated with 25 and 50 μg/mL 7 α,25-DHC for 48 h, respectively, compared with that of the control cells (101.1 ± 15.3%). These data indicate that 7α,25-DHC is a potential catabolic oxysterol that suppresses the synthesis of Col II and aggrecan, major components of articular cartilage.

III-4. 7α,25-DHC upregulates the expression and activity of cartilage-degrading enzymes in chondrocytes

Next, to verify the catabolic effects of 7α,25-DHC on the degeneration of articular cartilage as well as the expression and activation of cartilage-degrading enzymes such as MMP-13 and MMP-1, primary rat chondrocytes were cultured with 25 and 50 μ g/mL of 7α,25-DHC for 48 h. To assess the alteration of MMPs, qPCR, qRT-PCR, western blotting, and gelatin zymography were performed, as shown in Fig. 5. The mRNA and protein levels of MMP-13 and MMP-3 increased significantly in the chondrocytes treated with 7α,25-DHC, as shown in Fig. 5A and 5B. Furthermore, the results of qRT-PCR showed that the induction of MMP-3 mRNA increased 49 ± 3.1- and 64.3 ± 7.3-fold in chondrocytes treated with 25 and 50 μg/mL 7α,25-DHC, respectively, compared with that of the control cells (1 ± 0.1-fold), as shown in Fig. 5C. In addition, MMP-13 mRNA expression increased 11.2 ± 4.2- and 22.9 ± 9.2-fold in the chondrocytes treated with 25 and 50 μg/mL 7α,25-DHC, respectively, compared with that of the control cells (1.1 ± 0.6-fold). As shown in Fig. 5D, the activity of matrix-degrading enzymes increased in a dose-dependent manner in chondrocytes treated with 25 and 50 μg/mL 7α,25-DHC. These data indicate that 7α,25-DHC upregulates the expression and activity of cartilage-degrading enzymes in primary rat chondrocytes and that 7α,25-DHC is a potential catabolic oxysterol that induces the progressive degeneration of articular cartilage through the increased expression and activation of cartilage-degrading enzymes, such as MMP-13 and MMP-3, in chondrocytes.

III-5. 7α,25-DHC induces catabolic inflammatory mediators associated with oxidative stress

To verify whether 7α,25-DHC induces catabolic inflammatory mediators associated with oxidative stress, primary rat chondrocytes were cultured with 25 and 50 μg/mL of 7α,25-DHC for 48 h. Thereafter, mRNA and protein levels of catabolic inflammatory mediators, such as iNOS, COX-2, and PTGS2, were assessed by qPCR, western blotting, and qRT-PCR. As shown in Fig. 6A and 6B, mRNA and protein levels of iNOS, COX-2, and PTGS2 significantly increased in chondrocytes treated with 25 and 50 μg/mL of 7α,25-DHC. As shown in Fig. 6C, the mRNA levels of iNOS were 28.1 ± 4.4- and 48.9 ± 7.4-fold higher in chondrocytes treated with 25 and 50 μg/mL 7 α,25-DHC, respectively, compared with that of the control cells (1 ± 0.2-fold). COX-2 mRNA increased by 8.7 ± 1.1 and 12.1 ± 1.7 folds in the chondrocytes treated with 25 and 50 μg/mL 7α,25-DHC, respectively, compared with that of the control cells (1 ± 0.1%). Furthermore, as shown in Fig. 6D, the production of PGE_2 significantly increased by 527.9 ± 14.5 and 439.9 ± 12.9 pg/mL in the chondrocytes treated with 25 and 50 μg/mL 7α,25-DHC, respectively, compared with that of the control cells (152.2 ± 46.5 pg/mL). Moreover, the relative production of NO increased by 483.6 ± 12.4% and 592.7 ± 11.9% in the chondrocytes treated with 25 and 50 μg/mL 7 α,25-DHC, respectively, compared with that of control cells (100 ± 2.8%), as shown in Fig. 6E. These data indicate that 7α,25-DHC is a potential catabolic oxysterol that induces catabolic inflammatory mediators associated with oxidative stress and a catabolic factor that induces the progressive degeneration of articular cartilage.

III-6. 7α,25-DHC induces apoptotic cell death in chondrocytes

To investigate whether 7α,25-DHC is a toxic oxysterol in chondrocytes, primary rat chondrocytes were treated with 1, 10, 25, and 50 μg/mL 7α,25-DHC for 48 h. As shown in Fig. 7A, relative cell viability was 97.6 ± 1.3%, 75.9 ± 1%, 75.2 ± 1.5%,

and 67.9 ± 0.8% in the chondrocytes treated with 1, 10, 25, and 50 μg/mL 7α,25-DHC, respectively compared with that of the untreated control (100 ± 1.5%). Furthermore, the results of H&E staining showed that the number of chondrocytes decreased in a dose-dependent manner with 25 and 50 μg/mL 7α,25-DHC treatment compared with that of the untreated control, as shown in Fig. 7B (upper panel). Moreover, chondrocyte survival, measured using a cell Live/Dead assay, showed that the number of living chondrocytes decreased with 7α,25-DHC treatment in a dose-dependent manner, as shown in Fig. 7B (middle panel). In addition, the results of DAPI staining showed that the number of chondrocytes with condensed chromatin, a typical feature of apoptosis, increased with 7α,25-DHC treatment in a dose-dependent manner, as shown in Fig. 7B (lower panel). Taken together, these data indicate that 7α,25-DHC is a toxic oxysterol and induces apoptotic cell death in chondrocytes in a dose-dependent manner.

III-7. 7α,25-DHC increases the apoptotic population in chondrocytes

Next, to verify whether 7α,25-DHC-induced cell death involved apoptosis in chondrocytes, primary rat chondrocytes were cultured with 25 and 50 μg/mL of 7α,25-DHC for 48 h. Thereafter, the apoptotic population was assessed by FACS analysis using Annexin V and PI staining. As shown in Fig. 8, the relative rates of cell death were 40.87% and 82.61% in the chondrocytes treated with 25 and 50 μg/mL 7α,25-DHC, respectively. Furthermore, the population of early-stage apoptotic cells was 12.8% and 10.82% and that of late-stage apoptotic cells was 27% and 68.47% in chondrocytes treated with 25 and 50 μg/mL 7α,25-DHC, respectively. The necrotic cell population was 1.59% and 3.32% in chondrocytes treated with 25 and 50 μg/mL 7α,25-DHC, respectively. Therefore, the FACS analysis indicated that 7α,25-DHC-induces apoptotic cell death in chondrocytes.

III-8. 7α,25-DHC-induced cell death is dose-dependent and is mediated by extrinsic and intrinsic apoptosis in chondrocytes

To investigate 7α,25-DHC-induced chondrocyte death, western blot analyses were performed using antibodies against molecules involved in receptor-mediated extrinsic and mitochondria-dependent intrinsic apoptosis, as shown in Fig. 9. The expression of FasL was significantly upregulated in the chondrocytes treated with 25 and 50 μg/mL 7α,25-DHC, as shown in Fig. 9A. Additionally, the expression of both pro- and cleaved caspase-8 increased with 7α,25-DHC treatment in a dose-dependent manner. These results indicate that 7α,25-DHC-induced apoptosis is coordinated by an extrinsic death receptor-mediated apoptotic pathway through FasL and caspase-8 in chondrocytes. Furthermore, the expression of anti-apoptotic factors, such as BcL-2 and BcL-xL, decreased dose-dependently in response to 7α,25-DHC treatment in chondrocytes. In addition, in chondrocytes, the expression of Bid, a precursor of truncated Bid (tBid) that acts as a pro-apoptotic factor was decreased by 7α,25-DHC treatment in a dose-dependent manner, as shown in Fig. 9B. In contrast, the expression of Bax, Bad, and cleaved caspase-9, the pro-apoptotic factors associated with the mitochondria-dependent intrinsic apoptosis pathway, increased in chondrocytes treated with 25 and 50 μg/mL 7α,25-DHC, as shown in Fig. 9B. These results indicate that 7α,25-DHC-induced chondrocyte apoptosis is mediated by the mitochondria-dependent intrinsic apoptosis pathway and involves the downregulation of anti-apoptotic factor expression, upregulation of pro-apoptotic factor expression, and activation of caspase-9. As shown in Fig. 9C, the expression of cleaved caspase-3 increased in chondrocytes treated with 25 and 50 μg/mL 7α,25-DHC, owing to the cleavage of pro-caspase-3, a downstream substrate of cleaved caspase-8 and cleaved caspase-9. Additionally, the expression of cleaved PARP, a downstream substrate of caspase-3, was increased in chondrocytes treated with 25 and 50 μg/mL 7α,25-DHC. 7α,25-DHC not only upregulated the expression of caspase-3 in both chondrocytes and *ex vivo* organ-cultured articular cartilage, as indicated by immunocytochemistry (Fig. 9D) and immunohistochemistry (Fig. 9E), respectively, but also increased the activity of

caspase-3 in chondrocytes, as shown in Fig. 9F. Taken together, these findings consistently indicate that 7α,25-DHC-induced chondrocyte death is coordinated by death receptor-mediated extrinsic and mitochondria-dependent intrinsic apoptosis through activation of the caspase cascade in chondrocytes.

III-9. 7α,25-DHC-induced cell death is involved in autophagy in chondrocytes

Autophagy is a protein-degradation process during which the constituents of cells are digested in lysosomes [26]. Therefore, to determine whether 7α,25-DHC-induced cell death is involved in autophagic cell death, a western blotting assay was used to measure the expression of several marker proteins of autophagy after exposure to chondrocytes treated with 25 and 50 μg/mL 7α,25-DHC for 48 h. As shown in Fig. 10A, the expression of LC3 and Beclin-1, the specific biomarkers associated with autophagy, was significantly increased in chondrocytes treated with 7α,25-DHC in a dose-dependent manner. Furthermore, the immunoreactivity of Beclin-1 increased by 25 and 50 μg/mL 7α,25-DHC in both chondrocytes and *ex vivo* organ-cultured articular cartilage, as indicated by the results of immunocytochemistry (Fig. 10B) and immunohistochemistry (Fig. 10C), respectively. These results indicate that 7 α,25-DHC-induced cell death is involved in autophagy in chondrocytes.

III-10. 7α,25-DHC induces oxiapoptophagy in articular cartilage dissected from knee joints with OA

To confirm whether 7α,25-DHC acts as a pathophysiological factor to induce the progressive degeneration of articular cartilage via inducing oxiapoptophagy in severely degenerated articular cartilage, OA mice were generated by surgically destabilizing the median meniscus (DMM) at the knee joint. Three (middle stage of OA) and eight weeks (terminal stage of OA) after surgery, the articular cartilage of the knee joint

was dissected, and safranin-O and fast green staining were performed to observe the proteoglycan in the articular cartilage. Subsequently, immunohistochemistry was performed to verify oxiapoptophagy by measuring the expression of CYP7B1 for the synthesis of 7α,25-DHC, caspase-3 for apoptosis, and beclin-1 for autophagy. As shown in Fig. 11, safranin-O & fast green staining showed that proteoglycan loss from articular cartilage significantly increased in accordance with the severity of degeneration at each stage of OA in the mice. The immunoreactivity of CYP7B1, caspase-3, and beclin-1 increased in the articular cartilage that exhibited severe proteoglycan loss due to DMM in the knee joint. Collectively, these results indicate that 7α,25-DHC induces oxiapoptophagy in the articular cartilage of the knee joint in OA.

IV. DISCUSSION

OA is one of the most common joint diseases; it causes chronic joint pain and results in the progressive degeneration of articular cartilage in synovial joints. Thus, OA is being considered a major global socio-economic problem to be addressed urgently, owing to the substantially increase in elderly population worldwide [27]. As the pathophysiological etiology of OA is multifactorial and associated with various risk factors such as aging, excessive joint movement, traumatic joint injury, individual genetic heredity, and obesity, the precise pathological mechanisms of OA remain largely unknown [28]. Hence, although several studies have been conducted to develop an effective therapeutic agent for patients with OA, there are no effective medications [29]. Recent meta-analyses have suggested the pathophysiological linkages between metabolic syndromes, a cluster of the conditions of abdominal obesity, high blood pressure, high blood sugar, high serum triglycerides, low serum high-density lipoproteins, and arthritis, including OA and rheumatoid arthritis (RA) [30]. Although in vivo animal models with obesity, diabetes, or dyslipidemia have helped to better the understating of the pathophysiological linkage between metabolic syndromes and arthritis, the mechanism by which metabolic diseases induce the progressive degeneration of articular cartilage in synovial joints remains largely unknown [31].

Obesity is closely associated with the etiology of both metabolic syndromes and OA. Obesity increases joint loading due to excessive body weight and results in the progressive degeneration of articular cartilage due to its deleterious effects on weight-bearing joints [32]. Furthermore, obesity induces chronic inflammation and cell death via the production of adipokines in adipose tissues, which occurs under the hypoxic conditions resulting from hypertrophy and hyperplasia in response to excessive nutrition [33]. Hence, obesity is a catabolic risk factor of OA, owing to mechanical overload, increased inflammation, and the induction of chondrocyte death in the articular cartilage of synovial joints [34]. However, although these factors provide a part of the pathophysiological linkage between metabolic syndromes and

OA, there remains a need for a better understanding of the metabolic cellular mechanisms of the development of OA.

Oxysterols are cholesterol derivatives synthesized by the oxidation of cholesterol through enzymatic or radical processes [35]. Pathophysiological studies have reported that oxysterol is closely associated with tumor formation in breast cancer, neurodegenerative diseases such as Parkinson's disease and Alzheimer's disease, atherosclerosis, and apoptosis [36,37]. Recent studies have reported that some oxysterols, such as 25-HC, 7-ketocholesterol, 7β-hydroxycholesterol, and cholestane-3 β,5α,6β-triol, induce apoptosis in various types of cells, such as smooth muscle cells derived from rat aorta, human monocytic cell lines such as U-937 and HL-60, human keratinocytes, human head and neck carcinoma cell FaDu, cellosaurus cell line ECV-304, and human lymphoblastic leukemic CEM cells [25,38-42]. More recently, Seo et al. reported that 25-HC induces apoptosis in chondrocytes, which is a representative pathogenesis of OA [25]. Moreover, a recent study reported that the CH25H-CYP7B1-RORα axis regulates OA [43]. Taken together, these data suggest that oxysterol is closely involved in the pathophysiological etiology of metabolic OA [25]. Therefore, to investigate the pathophysiological linkage between metabolic syndromes and OA, it was hypothesized that 7α,25-DHC, a downstream oxysterol synthesized by CYP7B1 from 25-HC under inflammatory conditions, may be a metabolic risk factor associated with OA.

DHCs, such as 7α,25-DHC and 7α,27-DHC, are synthesized from cholesterol by the enzymes CH25H, CYP7B1, and CYP27A1 in inflammatory conditions. Hence, to verify the expression of these enzymes associated with 25-HC and 7α,25-DHC in chondrocytes under inflammatory conditions, chondrocytes were stimulated with LPS to induce inflammation. As shown in Fig. 2, LPS-induced inflammation suppressed the synthesis of extracellular matrix components such as aggrecan and Col II. Moreover, LPS-induced inflammation not only upregulated the expression of

cartilage-degrading enzymes such as MMP-13 and MMP-3, inflammatory mediators such as iNOS and COX-2, and the apoptosis of chondrocytes, but also increased the expression of oxysterol synthases such as CH25H and CYP7B1 in chondrocytes. Collectively, these data indicate that inflammation-induced catabolic conditions and apoptosis are involved in oxysterol synthesis in chondrocytes.

Previously, Seo et al. reported that 25-HC is a pathophysiological oxysterol associated with the acceleration of proteoglycan loss from articular cartilage due to the increased death of chondrocytes [25]. Hence, alterations in the extracellular matrix were investigated in both *ex vivo* organ-cultured articular cartilage and chondrocytes treated with or without 7α,25-DHC. As shown in Fig. 3 and Fig. 4, 7α,25-DHC not only accelerated proteoglycan loss in articular cartilage, but also suppressed the mRNA induction of aggrecan and Col II, the major components of the extracellular matrix. Hence, these data indicate that 7α,25-DHC is a pathophysiological oxysterol that induces the progressive degeneration of articular cartilage through the acceleration of proteoglycan loss and suppression of ECM components.

The progressive degeneration of articular cartilage and eventual complete loss of chondrocytes are the major clinical symptoms of OA [44]. Cartilage-degrading enzymes, including MMP-13 and MMP-3, are responsible for the progressive degeneration of articular cartilage during OA pathogenesis [45]. Hence, biochemical therapeutic strategies to attenuate or prevent OA include the inhibition of both the expression and activation of cartilage-degrading enzymes. However, Tomohiro et al. reported that 25-HC promotes fibroblast-mediated tissue remodeling via the upregulation of MMP-2 and MMP-9 in chronic obstructive pulmonary disease [46]. In the present study, the expression and activity of cartilage-degrading enzymes such as MMP-13 and MMP-3 significantly increased in the conditioned media harvested from chondrocytes treated with 7α,25-DHC, as shown in Fig. 5. These data indicate that 7α,25-DHC is a pathophysiological oxysterol that accelerates the digestion of

ECM through the upregulation of cartilage-degrading enzymes, in a manner similar to that of 25-HC.

Inflammatory mediators, such as iNOS, COX-2, NO, and PGE_2, are representative catabolic factors associated with the upregulation of cartilage-degrading enzymes and proteoglycan loss due to the increased production of pro-inflammatory cytokines, such as IL-1β, IL-6, and TNF-α, during OA progression [47]. Recent studies have shown that 25-HC is closely associated with the inflammatory response. Pokharel et al. reported that 25-HC increases the production of pro-inflammatory cytokines such as TNF-α and IL-6 via activating α5β1 and αvβ3 integrin in macrophages and epithelial cells [48]. Jang et al. reported that 25-HC contributes to cerebral inflammation and increases oligodendrocyte cell death via activating the NLRP3 inflammasome [49]. In the present study, the expression and production of inflammatory mediators that act as catabolic risk factors of OA increased significantly in chondrocytes treated with 7 α,25-DHC, as shown in Fig. 6. These data suggest that 7α,25-DHC is a pathophysiological oxysterol that upregulates the inflammatory mediators associated with oxidative stress to induce the production of pro-inflammatory cytokines during OA progression.

Apoptosis is a highly regulated form of cell death [50]. However, the dysregulation of apoptosis is a pathophysiological risk factor for the induction of cancer, developmental abnormalities, and degenerative diseases including OA [51]. In particular, chondrocytes are closely associated with the ECM maintenance. Hence, chondrocyte apoptosis leads to the progressive degeneration of articular cartilage due to the imbalance between anabolism and catabolism [52]. Furthermore, chondrocyte apoptosis occurs frequently in osteoarthritic cartilage. Recently, Seo et al. reported that 25-HC induced the apoptosis of chondrocytes via FasL-triggered extrinsic and mitochondria-dependent intrinsic apoptosis [25]. As shown in Fig. 7-9, 7α,25-DHC increased caspase-dependent apoptotic cell death through FasL-triggered extrinsic and mitochondria-dependent intrinsic apoptosis, showing similarity with 25-HC-induced

apoptosis, in chondrocytes. These data consistently indicate that 7α,25-DHC is a pathophysiological oxysterol that induces OA by increasing apoptotic cell death in chondrocytes.

Autophagy is an important physiological process that degrades intracellular components, such as unnecessary or damaged cellular organelles and protein aggregates, in all living cells and transports them to lysosomes for recycling [53]. LC3 and Beclin-1 are common biomarkers of autophagy. During autophagy activation, LC3B is cleaved into LC3II and localizes to the autophagosome membrane, where it plays a role in initiating autophagosome formation [54]. Beclin-1 participates in the autophagy by regulating phosphatidylinositol 3-phosphate and the recruiting autophagy-related proteins, which are essential for the formation of pre-autophagosomal structures [55]. Studies have reported that oxysterol induces autophagy in various types of cells, such as vascular smooth muscle cells and murine oligodendrocytes [20]. Hence, to verify whether 7α,25-DHC-induced cell death is involved with autophagy, the alteration of biomarkers associated with autophagy was investigated, as shown in Fig. 10. The expression of Beclin-1 and LC3, biomarkers associated with autophagy, significantly increased by 7α,25-DHC in chondrocytes. These data suggest that 7α,25-DHC-induced cell death is involved in apoptosis accompanied by autophagy and this process is known as oxiapoptophagy.

To confirm 7α,25-DHC-induced oxiapoptophagy in osteoarthritic cartilage, OA mice were generated via surgical DMM at the knee joint [56]. To evaluate oxiapoptophagy in accordance with OA severity, OA animals were sacrificed three (middle stage of OA) and eight weeks (terminal stage of OA) after DMM surgery. As shown in Fig. 11, the immunoreactivity of CYP7B1, caspase-3, and beclin-1 increased in the articular cartilage that exhibited severe proteoglycan loss due to DMM in the knee joint. These data consistently indicate that 7α,25-DHC-induced cell death is involved in oxiapoptophagy in the articular cartilage of the knee joint in OA.

Collectively, the present study clearly demonstrated that 7α,25-DHC, a pathophysiological oxysterol that induces OA, causes an increase in catabolic factors, including the expression of cartilage-degrading enzymes and the production of inflammatory mediators, and induces the oxiapoptophagy of chondrocytes. To fully understand metabolic OA, further investigations are warranted to elucidate the pathophysiological roles of 7α,25-DHC in animals with metabolic syndromes and OA. However, this study has provided insight into the pathophysiological linkage between metabolic syndrome and OA that involves 7α,25-DHC.

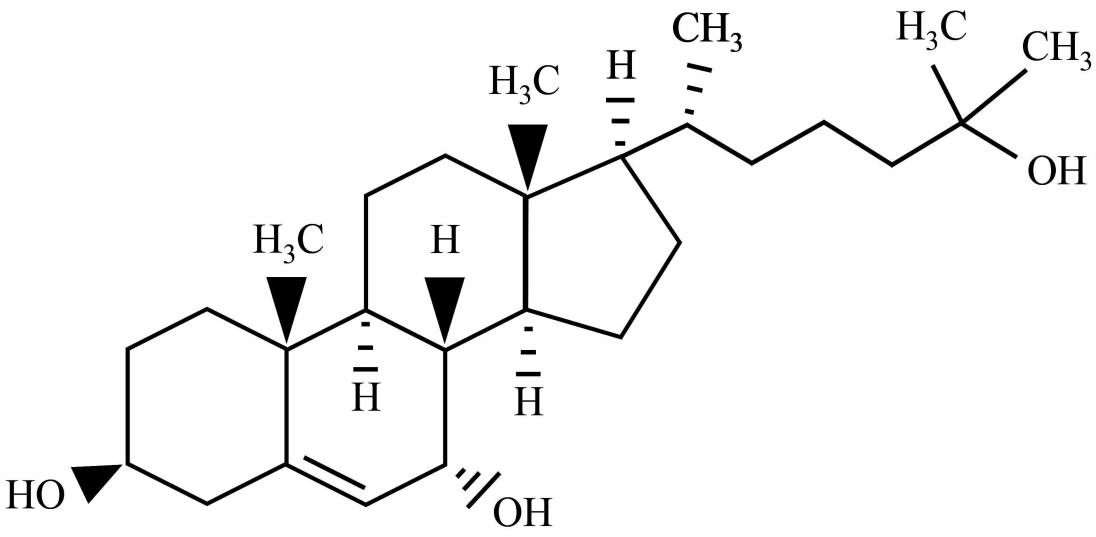

7α,25-Dihydroxycholesterol

- Other names : 7α,25-dihydroxycholesterol, Cholest-5-ene-3β, 7α,25-triol, 7-α,25-dihydroxycholesterol, 5-cholesten-3β, 7α,25-triol
- Chemical formula : $C_{27}H_{46}O_3$
- Molecular weight : 418.65
- CAS NO. 64907-22-8
- IUPAC name : (3*S*,7*S*,8*S*,9*S*,10*R*,13*R*,14*S*,17*R*)-17-[(2*R*)-6-hydroxy-6-methylheptan-2-yl]-10,13-dimethyl-2,3,4,7,8,9,11,12,14,15,16,17-dodecahydro-1*H*-cyclopenta[a]phenanthrene-3,7-diol

Figure 1. Chemical structure of 7α,25-DHC.

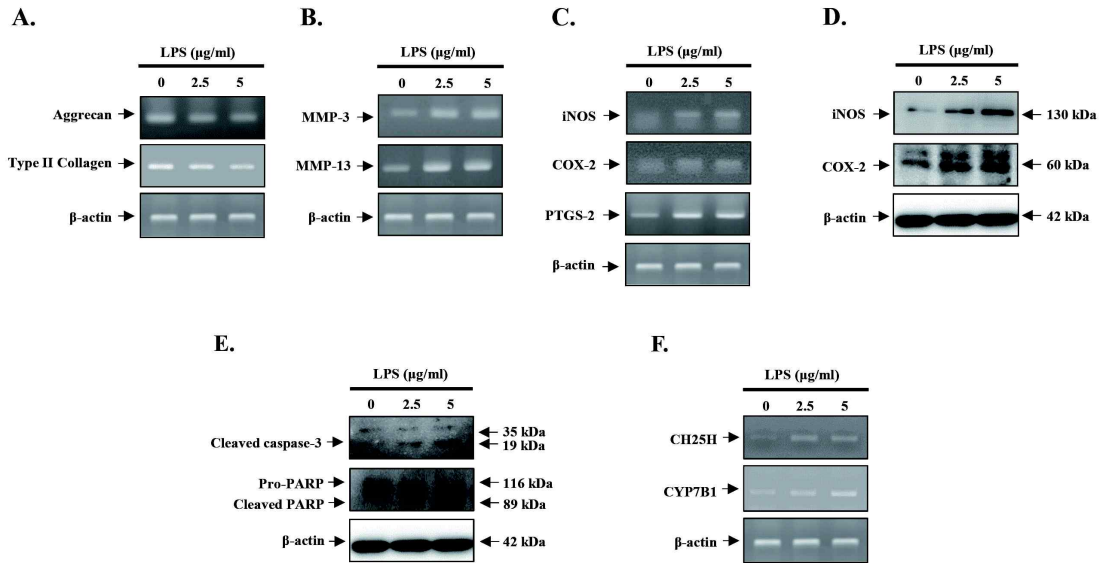

Figure 2. LPS-induced inflammation increased catabolic effects and induced the expression of oxysterol synthase in chondrocytes. Primary rat chondrocytes were treated with 2.5 and 5 μg/mL LPS for 48 h. Total RNA and cell lysates were prepared to perform qPCR to investigate the mRNA induction of aggrecan, Col II, MMP-3, MMP-13, iNOS, COX-2, PTGS-2, CH25H, and CYP7B1, and western blot was performed using specific antibodies against caspase-3, PARP, CH25H, and CYP7B1. A, mRNA levels of aggrecan and Col II, major components of the extracellular matrix, decreased dose-dependently by LPS in chondrocytes. B, mRNA levels of MMP-3 and MMP-13, representative cartilage-degrading enzymes, were increased dose-dependently by LPS in chondrocytes. C & D, mRNA (C) and protein levels (D) of iNOS, COX-2, and PTGS-2, catabolic inflammatory mediators associated with oxidative stresses, were increased dose-dependently by LPS. E, expression of pro-apoptotic factors, such as caspase-3 and PARP, was increased by LPS. F & G, mRNA (F) and protein (G) levels of cholesterol-25-hydroxylase (CH25H) and CYP7B1 significantly increased in the chondrocytes treated with LPS.

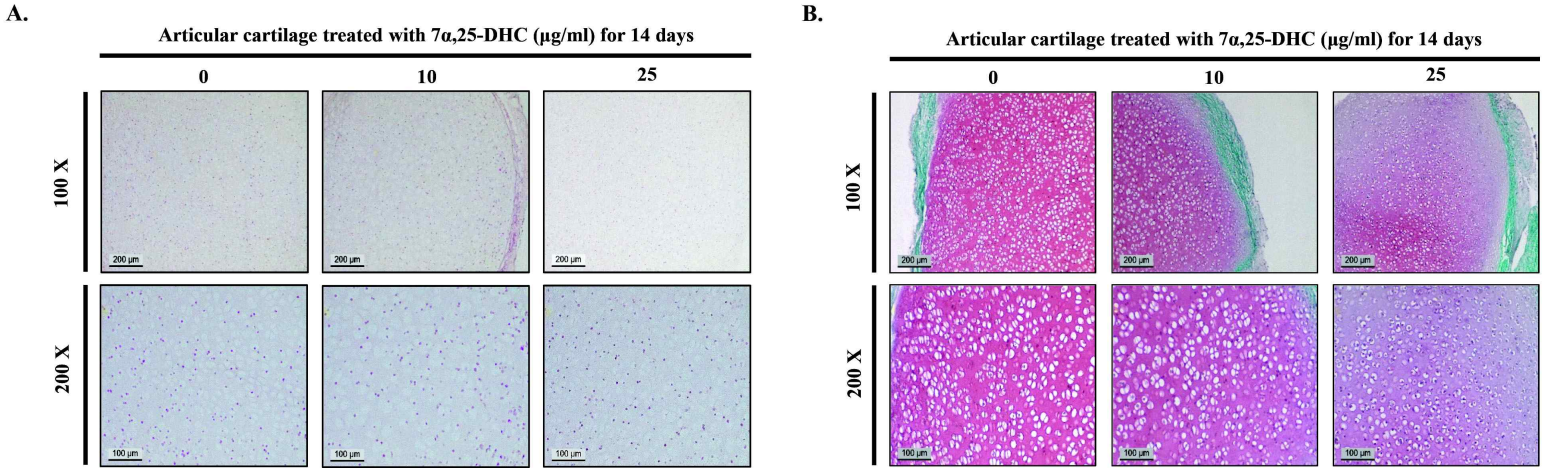

Figure 3. 7α,25-DHC accelerated proteoglycan loss in articular cartilage. Explants of articular cartilage dissected from the knee joint of 5-day-old rats were *ex vivo* organ-cultured with 10 and 25 μg/mL of 7α,25-DHC for 14 days. Thereafter, explants of articular cartilage were fixed with 4% paraformaldehyde for one week and then embedded into paraffin to perform hematoxylin and eosin staining (A) as well as safranin-O and fast green staining (B). A, 7α,25-DHC did not affect the morphological changes in articular cartilage. B, proteoglycan loss was increased dose-dependently by 7α,25-DHC in the explant of articular cartilage dissected from the knee joint of 5-day-old rats.

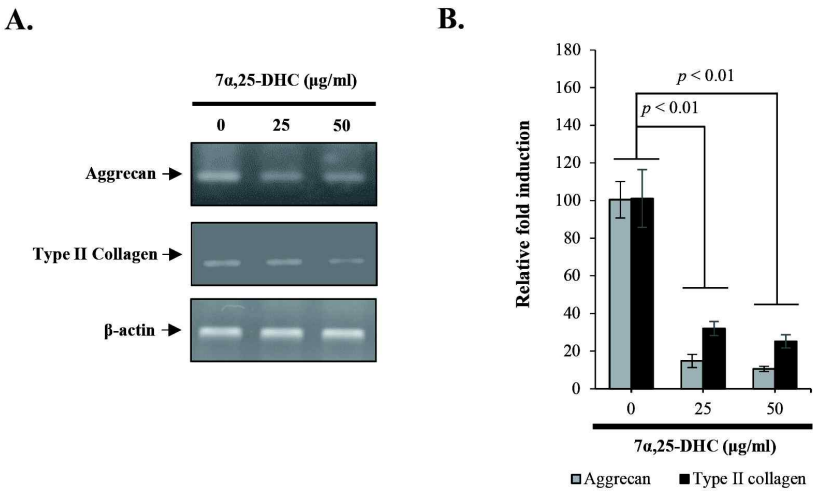

Figure 4. 7α,25-DHC suppressed the mRNA induction of Col II and aggrecan in chondrocytes. Primary rat chondrocytes were treated with 25 and 50 μg/mL of 7α,25-DHC for 48 h. Thereafter, cDNA was synthesized from isolated total RNA to perform qPCR (A) and qRT-PCR (B). A & B, mRNA levels of aggrecan and Col II, major components of the extracellular matrix, decreased by 7α,25-DHC in chondrocytes. The data are expressed as the mean ± standard deviation (SD; $p < 0.05$ and $p < 0.01$, respectively).

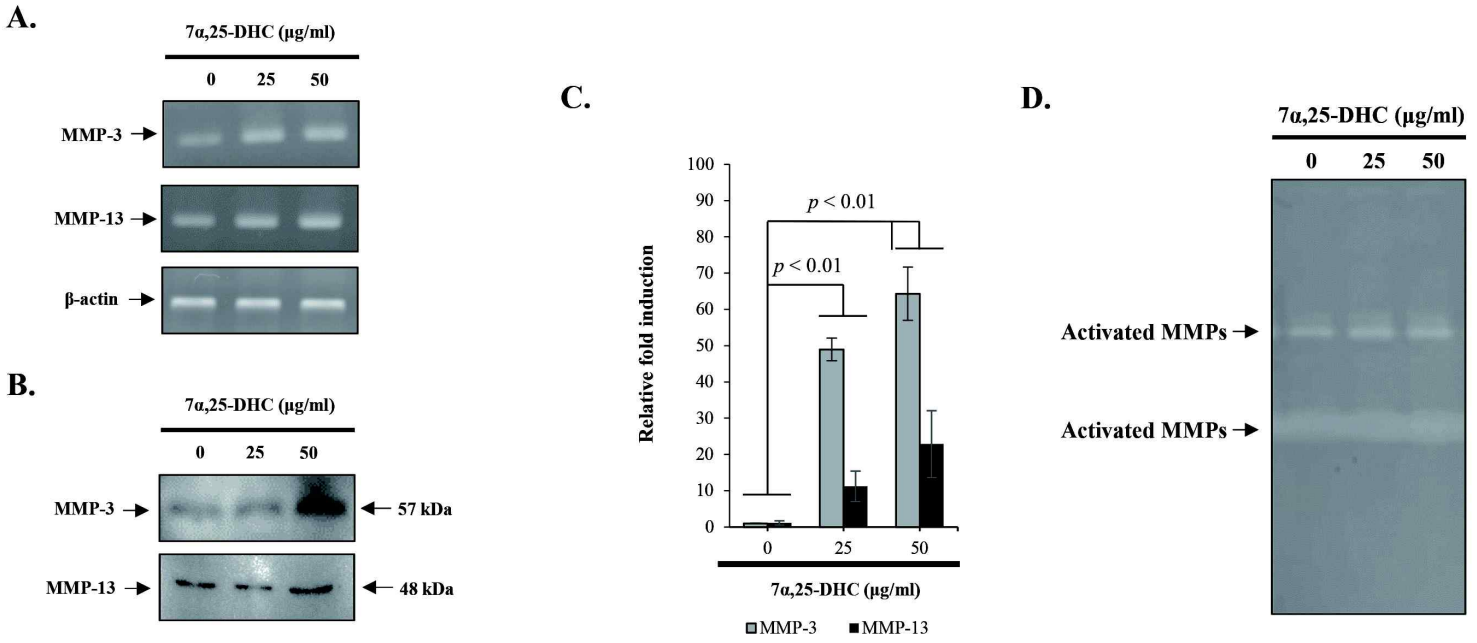

Figure 5. 7α,25-DHC upregulated the expression and activity of cartilage-degrading enzymes in chondrocytes. Primary rat chondrocytes were treated with 25 and 50 μg/mL of 7α,25-DHC for 48 h. Thereafter, the expression and activation of matrix metalloproteinase were assessed by qPCR (A), western blot (B), qRT-PCR (C), and gelatin zymography (D). A-C, mRNA (A & C) and protein (B) levels of MMP-3 and MMP-13 were increased by 7α,25-DHC dose-dependently in chondrocytes. D, the activity of cartilage-degrading enzymes increased in the conditioned media of chondrocytes treated with 25 and 50 μg/mL 7 α,25-DHC. The data are expressed as the mean ± standard deviation (SD; $p < 0.05$ and $p < 0.01$, respectively).

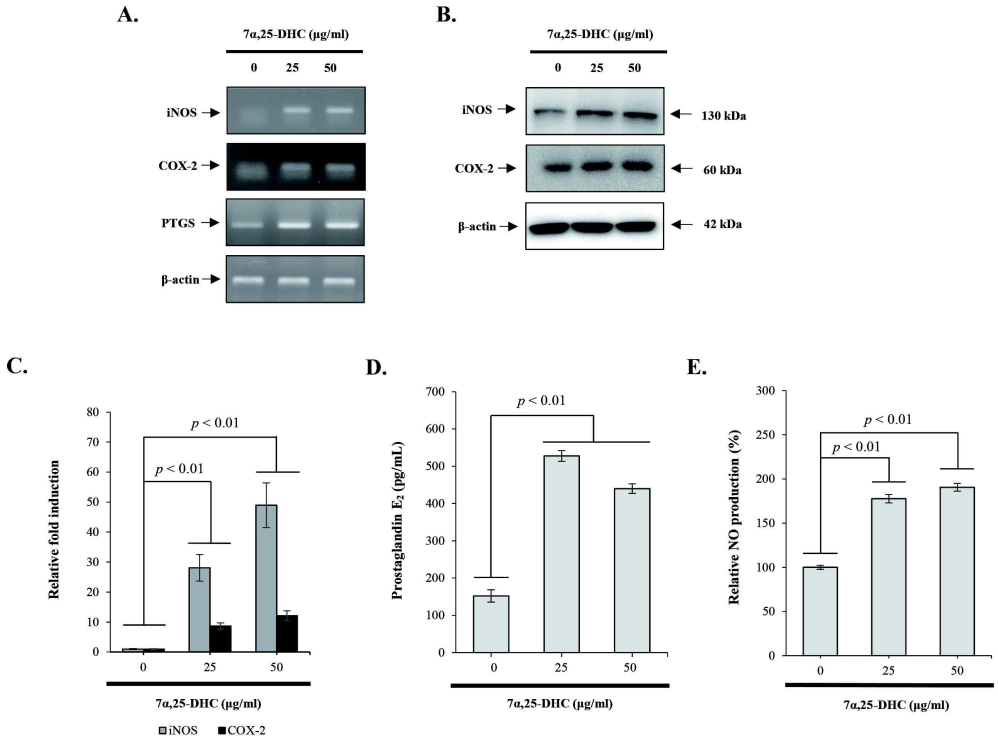

Figure 6. 7α,25-DHC induced catabolic inflammatory mediators associated with oxidative stress. Primary rat chondrocytes were treated with 25 and 50 μg/mL of 7α,25-DHC for 48 h. Thereafter, qPCR (A), western blot (B), qRT-PCR (C), and ELISA for PGE_2 (D) and NO (E) were performed to assess the catabolic inflammatory mediators associated with oxidative stress. A-C, the mRNA (A&C) and protein (B) levels of catabolic inflammatory mediators such as iNOS, COX-2, and PTGS-2 increased dose-dependently in chondrocytes treated with 7α,25-DHC. D & E, the production of PGE_2 (D) and NO (E) was increased dose-dependently by 7α,25-DHC in chondrocytes. The data are expressed as the mean ± standard deviation (SD; $p < 0.05$ and $p < 0.01$, respectively).

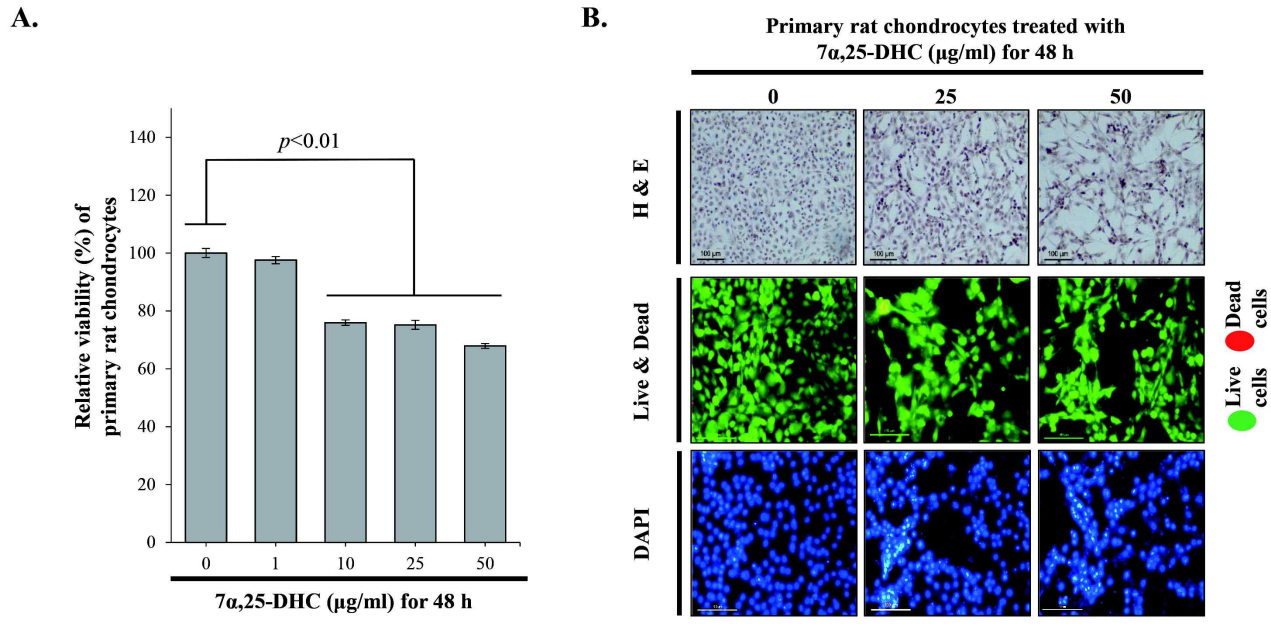

Figure 7. 7α,25-DHC induced apoptotic cell death in chondrocytes. Primary rat chondrocytes were treated with 1, 10, 25, and 50 μg/mL of 7α,25-DHC for 48 h. Cytotoxicity was measured using the MTT assay. H&E staining (upper B), cell Live/Dead assay (middle of B), and DAPI staining (lower B) were performed to investigate the morphological alteration, cell survival, and chromatin condensation, respectively, in chondrocytes treated with 25 and 50 μg/mL 7α,25-DHC for 48 h. Images were captured by fluorescence microscopy (Eclipse TE2000; Nikon Instruments, Melville, NY, USA). The data are expressed as the mean ± standard deviation (SD; $p < 0.05$ and $p < 0.01$, respectively).

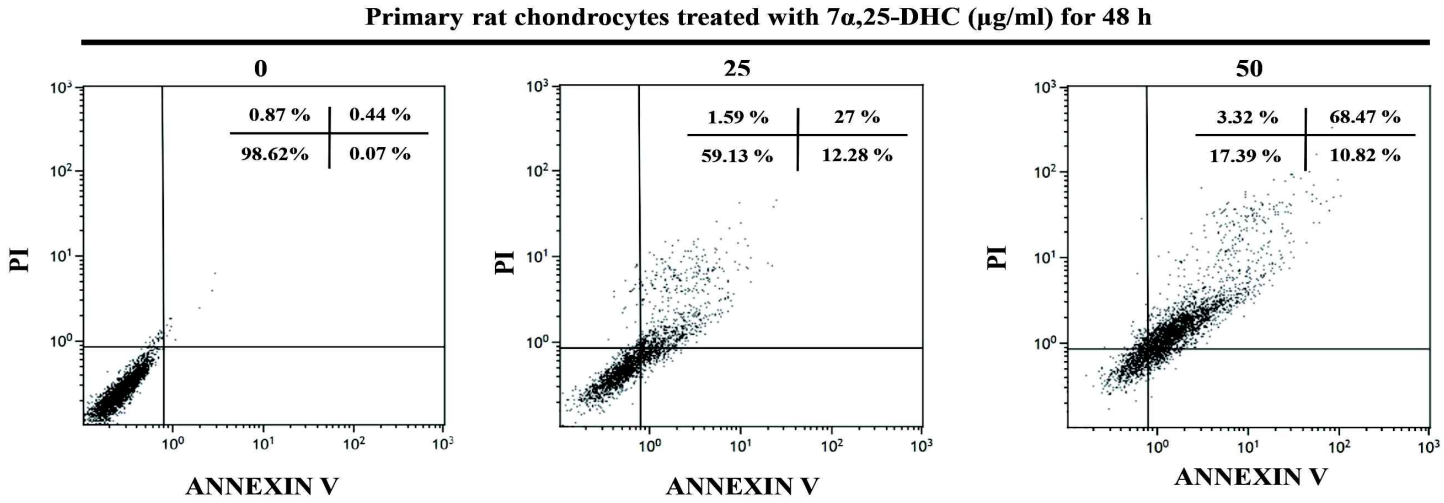

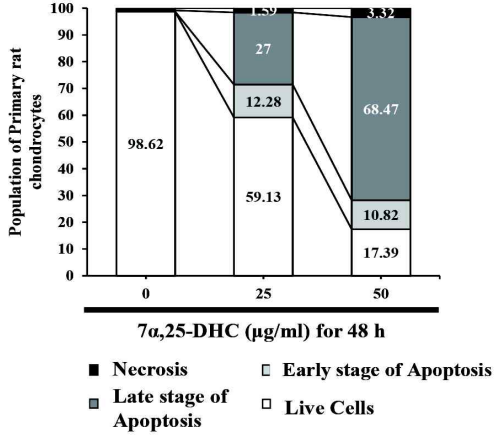

Figure 8. 7α,25-DHC increased the apoptotic population in chondrocytes. Primary rat chondrocytes were treated with 25, and 50 μg/mL 7α,25-DHC for 48 h. Thereafter, FACS analysis was performed to measure the apoptotic population

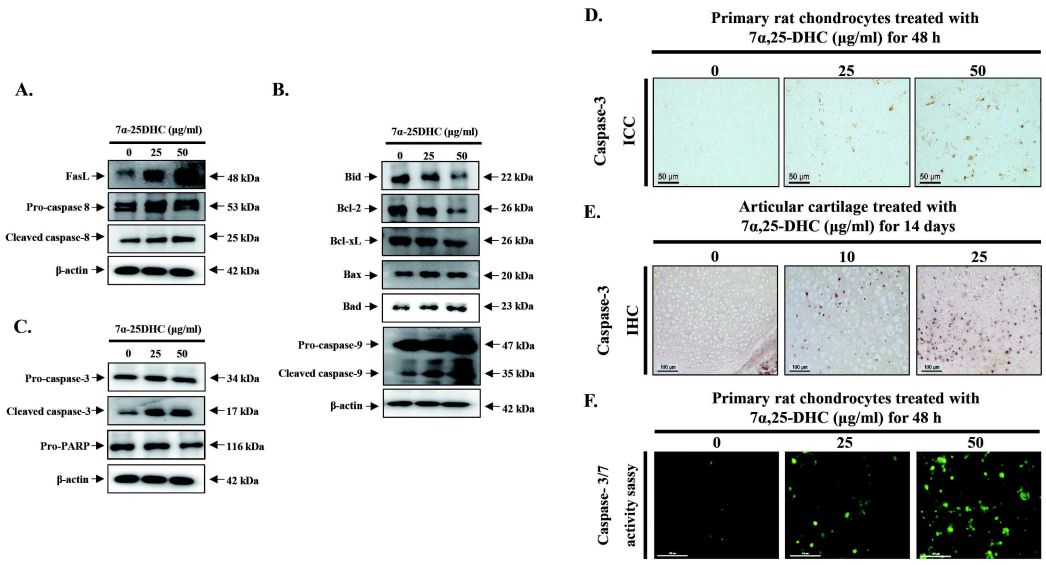

Figure 9. 7α,25-DHC-induced cell death was mediated caspase-dependently by extrinsic and intrinsic apoptosis in chondrocytes. Primary rat chondrocytes were treated with 25 and 50 μg/mL 7α,25-DHC for 48 h. Thereafter, western blot (A) using pro-apoptotic and anti-apoptotic antibodies, immunocytochemistry (B) using caspase-3 antibody, and caspase-3/-7 activity assay using cell-permeable fluorogenic substrate caspase-3/-7 substrate solution were performed to verify the apoptotic signaling pathways. Immunohistochemistry was performed to verify the expression of caspase-3 in the explant of articular cartilage treated with 10 and 25 μg/mL 7α,25-DHC for 14 days. A, 7α,25-DHC induced death receptor-mediated extrinsic apoptosis in chondrocytes, which was regulated by cleavage of caspase-8. B, 7α,25-DHC induced mitochondria-dependent intrinsic apoptosis via activating caspase-9 in chondrocytes. C, Caspase-3 was cleaved by both cleaved caspase-3 and PARP in chondrocytes. D & E, 7α,25-DHC induced the expression of caspase-3 in chondrocytes (D) and articular cartilage (E). F, Caspase-3/-7 activity was increased in the chondrocytes treated with 7α,25-DHC.

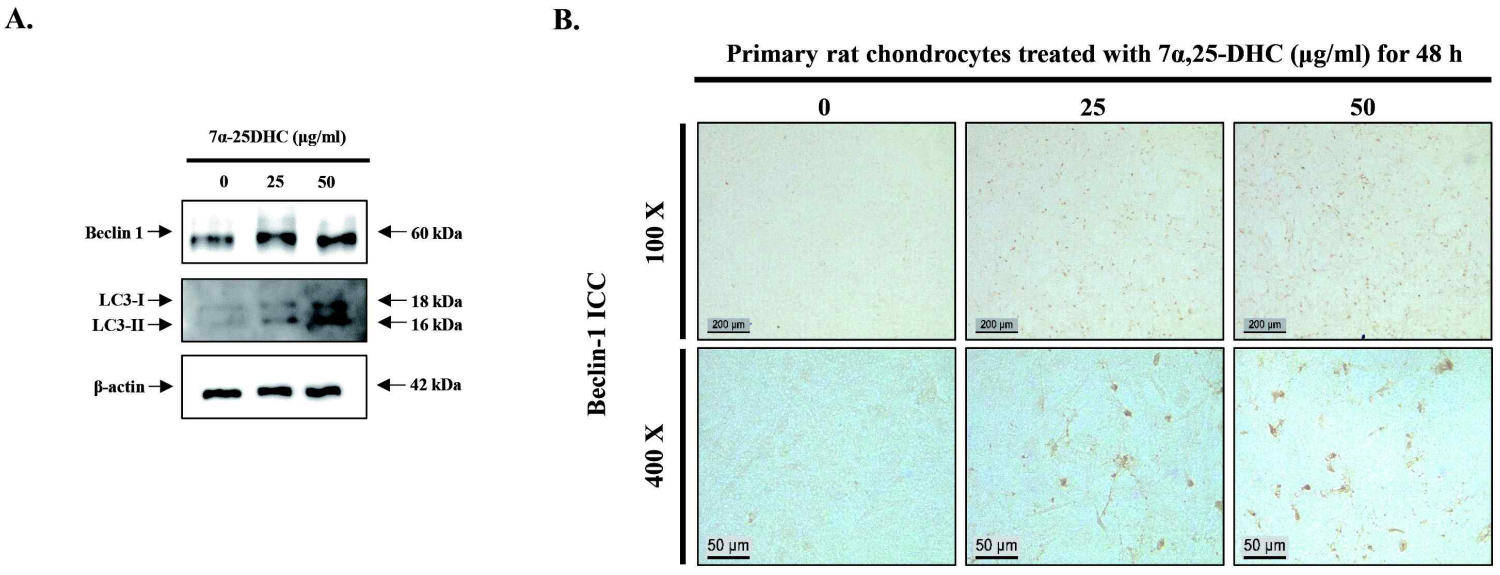

Figure 10. 7α,25-DHC-induced cell death is involved in autophagy in chondrocytes. Primary rat chondrocytes were treated with 25, and 50 μg/mL 7α,25-DHC for 48 h. Thereafter, western blot (A) was performed to verify the expression of Beclin-1 and LC3, biomarkers of autophagy. Immunocytochemistry (B) was performed to verify the expression of beclin-1 in the chondrocytes treated with 25 and 50 μg/mL 7α,25-DHC for 48 h. Immunohistochemistry (C) was performed to verify the expression of beclin-1 in the explant of articular cartilage treated with 10 and 25 μg/mL 7α,25-DHC for 14 days. A, the expression of Beclin-1 and LC-3 was upregulated in the chondrocytes treated with 7α,25-DHC. B & C, the immunoreactivity of Beclin-1 was increased by 7α,25-DHC in the chondrocytes (B) and explant of articular cartilage (C).

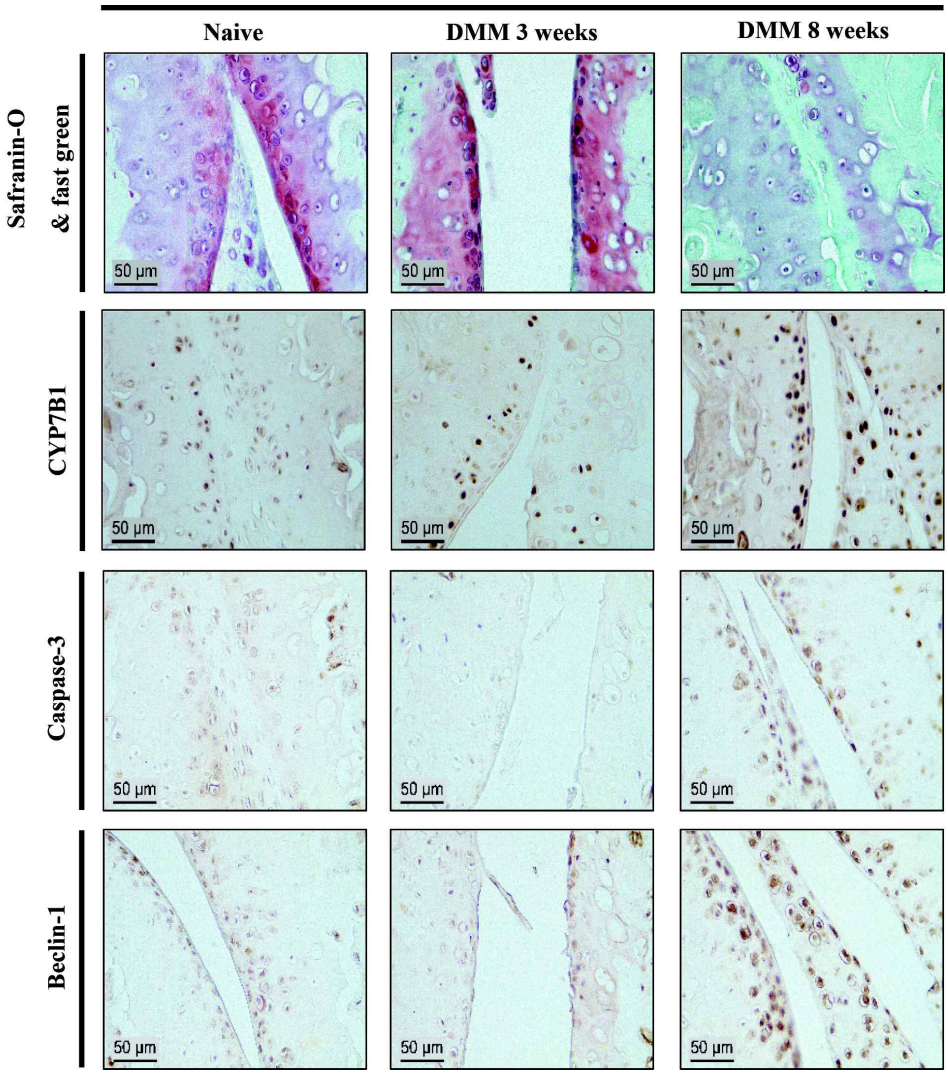

Figure 11. 7α,25-DHC induced oxiapoptophagy in the articular cartilage dissected from the knee joint with OA. OA mice were generated by the surgical destabilization of the median meniscus (DMM) at the knee joint. The knee joints were dissected three (middle stage of OA) and eight weeks (late stage of OA) after DMM surgery. Thereafter, safranin-O and fast green staining were performed to stain the proteoglycan in the articular cartilage. Subsequently, immunohistochemistry was performed to verify the expression of CYP7B1 for the synthesis of 7α,25-DHC, caspase-3 for apoptosis, and Beclin-1 for autophagy. In accordance with the increasing severity of proteoglycan loss, the immunoreactivity of CYP7B1, caspase-3, and Beclin-1 increased in the articular cartilage that exhibited severe proteoglycan loss due to DMM in the knee joint.

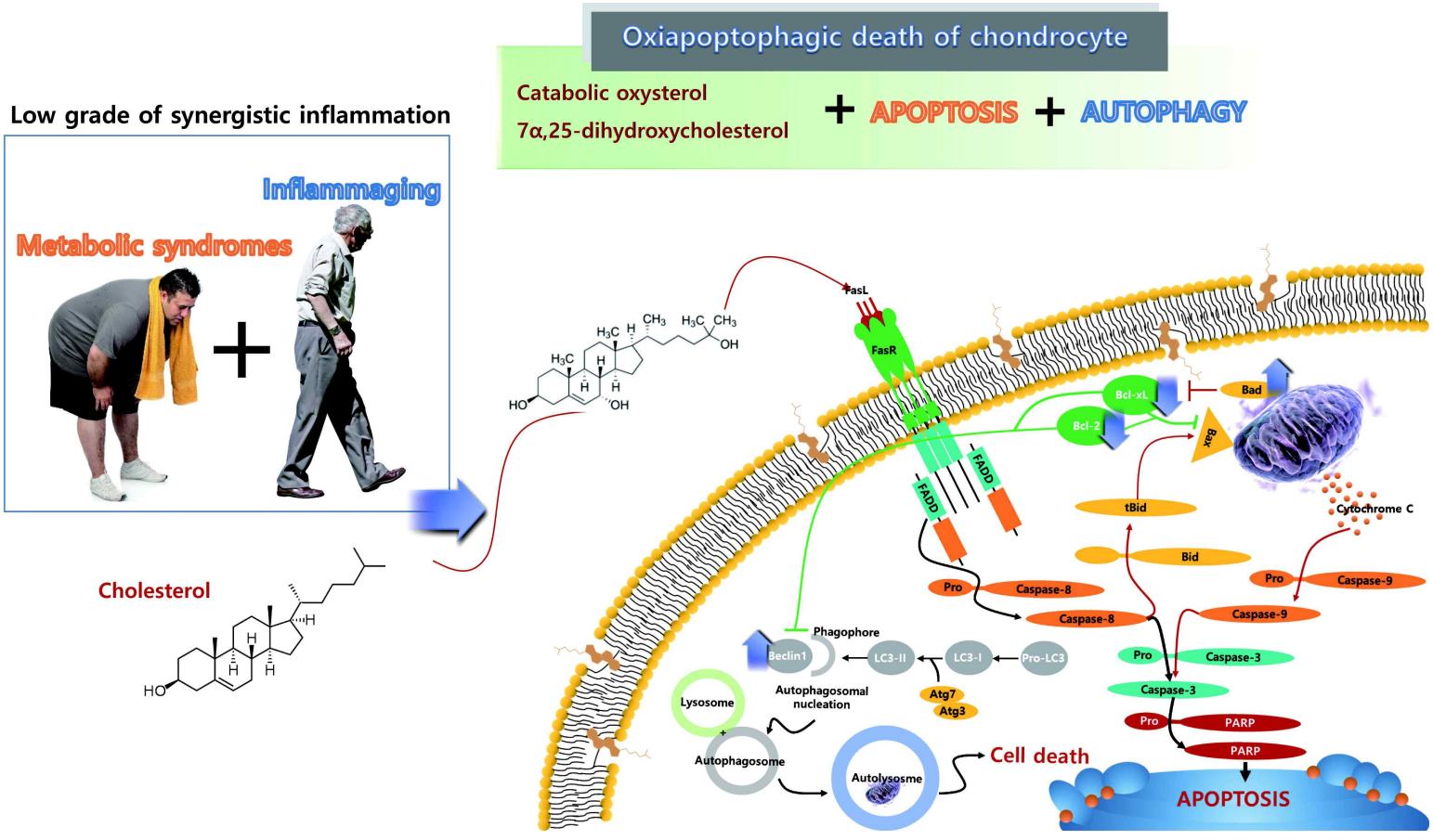

Figure 12. Schematic diagram of catabolic oxysterol 7α,25-DHC-induced oxiapoptophagic chondrocyte death in OA.

TABLE

Table 1. PCR primer sequences used in this study

qPCR	Gene	Primer sequences	NCBI gene no.
	ADAMTS4	Forward : 5'-GGTGCTTTGGCCACCTCAAT-3' Reverse : 5'-ACCACCTCCACAAGTCCTGG-3'	NM_023959.1
	ADAMTS5	Forward : 5'-ACACCTGCGTATTTGGGAACCCA-3' Reverse : 5'-GTGTCTGACCAAGAAGTTGCCTGC-3'	NM_198761.1
	Aggrecan	Forward : 5'-CAGAGGAACACACCGAAAGT-3' Reverse : 5'-GCACACTGGCTCCATCTATT-3'	NM_022190.1
	CH25H	Forward : 5'-CCCTTCTTCCCAGTCATCTTT-3' Reverse : 5'-TCCCAGACGCTCATGTATTG-3'	NM_001025415.1
	Col II	Forward : 5'-GGTCCTGGCATCGACAT-3' Reverse : 5'-GTGCGAGCGGGATTCTT-3'	NM_012929.1
	COX-2	Forward : 5'-CCCTTCCTCCTGTGGCTGAT-3' Reverse : 5'-CCCAGGTCCTCGCTTCTGAT-3'	NM_017232.3
	CYP7B1	Forward : 5'-CGGGCATGAAGAGTTTGAAATAG-3' Reverse : 5'-AGACTTCTGGGTCATTGTGTATC-3'	NM_019138.1
	INOS	Forward : 5'-GCATCGGCAGGATTCAGTGG-3' Reverse : 5'-TAGCCAGCGTACCGGATGAG-3'	NM_012611.3
	MMP3	Forward : 5'-TCCTACCCATTGCATGGCAGTGAA-3' Reverse : 5'-GCATGAGCCAAGACCATTCCAGG-3'	NM_133523.2
	MMP13	Forward : 5'-GGCAAAAGCCATTTCATGCTCCCA-3' Reverse : 5'-AGACAGCATCTACTTTGTCGCCA-3'	NM_133530.1
	PTGS2	Forward : 5'-ACTGGGCCATGGAGTGGACTTAAA-3' Reverse : 5'-TCAGTATGAGCCTGCTGGTTTGGA-3'	NM_017232.3
	β-actin	Forward : 5'-CGATAAAGGAAGGCTGGAAGAG-3' Reverse : 5'-GTGCCCATCTATGAGGGTTATG-3'	NM_019212.2

Table 2. Real -Time PCR primer sequences used in this study

qRT-PCR	Gene	Primer sequences	NCBI gene no.
	ADAMTS4	Forward : 5'-CTCTGGGTATGGCTGATGTG-3' Reverse : 5'-ACGGTTTGGAGTTATCATGGAG-3'	NM_023959.1
	ADAMTS5	Forward : 5'- GGGTTATACTGACGTTGTGAGG-3' Reverse : 5'-TCTAGTCTGGTCTTTGGCTTTG -3'	NM_011782.2
	Aggrecan	Forward : 5'-CCCCAAATCCCTCATACTCAG-3' Reverse : 5'-CTGTTTCTCCTGACCCTTCTG-3'	NM_032893390.1
	CH25H	Forward : 5'-CACTCACCATCCTCGTCTTTC-3' Reverse : 5'-GGAAAGTCGTAACCTGAGTGG-3'	NM_001025415.1
	Col II	Forward : 5'-AGCACATCTGGTTTGGAGAG-3' Reverse : 5'-CAGTGGTAGGTGATGTTCTGG-3'	NM_012929.1
	COX-2	Forward : 5'-CAACCCATGTCAAAACCGTG-3' Reverse : 5'-TTGTCAGAAACTCAGGCGTAG-3'	NM_017232.3
	CYP7B1	Forward : 5'-AATTGTTCAGGAGAGGCAGG-3' Reverse : 5'-CATAGCTGGAATGGTGTTTGC-3'	NM_019138.1
	iNOS	Forward : 5'-CGGTGTTCTTTGCTTCTGTG-3' Reverse : 5'-TGAAGGCGTAGCTGAACAAG-3'	NM_012611.3
	MMP3	Forward : 5'-GACCCTGAGACCT1TACCAATG-3' Reverse : 5'-AAAGAACAAGACTTCTCCCCG-3'	NM_133523.3
	MMP13	Forward : 5'-GATGAAGACCCCAACCCTAAG-3' Reverse : 5'-GGAGACTAGTAATGGCATCAAGG-3'	NM_133530.1
	GAPDH	Forward : 5'-ATGGGTGTGAATGAGAAGGAC-3' Reverse : 5'-GTCATTAGCCCTTCCACGATC-3'	NM_023964.1

Ⅴ. REFERENCES

[1] B. Calais-Germain, Anatomy of movement, Eastland Press1993.

[2] I. Khan, S. Redman, R. Williams, G. Dowthwaite, S. Oldfield, C.J.C.t.i.d.b. Archer, The development of synovial joints, 79 (2007) 1-36.

[3] R.J.C.p.d. Cancedda, Cartilage and bone extracellular matrix, 15 (2009) 1334-1348.

[4] C.R. Fellows, C. Matta, R. Zakany, I.M. Khan, A.J.F.i.g. Mobasheri, Adipose, bone marrow and synovial joint-derived mesenchymal stem cells for cartilage repair, 7 (2016) 213.

[5] P. Sarzi-Puttini, M.A. Cimmino, R. Scarpa, R. Caporali, F. Parazzini, A. Zaninelli, F. Atzeni, B. Canesi, Osteoarthritis: an overview of the disease and its treatment strategies, Seminars in arthritis and rheumatism, Elsevier, 2005, pp. 1-10.

[6] S.N. Lauder, Investigating the role of NF-κB in the pathology of osteoarthritis, Cardiff University (United Kingdom)2007.

[7] L. Duan, B. Ma, Y. Liang, J. Chen, W. Zhu, M. Li, D.J.A.j.o.t.r. Wang, Cytokine networking of chondrocyte dedifferentiation in vitro and its implications for cell-based cartilage therapy, 7 (2015) 194.

[8] M.B.J.C.r.r. Goldring, Osteoarthritis and cartilage: the role of cytokines, 2 (2000) 459-465.

[9] H. Kim, F.J.C.d.t. Blanco, Cell death and apoptosis in osteearthritic cartilage, 8 (2007) 333-345.

[10] P.A. Dieppe, L.S.J.T.L. Lohmander, Pathogenesis and management of pain in osteoarthritis, 365 (2005) 965-973.

[11] F. Salaffi, A. Ciapetti, M.J.R. Carotti, The sources of pain in osteoarthritis: a pathophysiological review, (2014) 57-71.

[12] B. Xia, D. Chen, J. Zhang, S. Hu, H. Jin, P.J.C.t.i. Tong, Osteoarthritis pathogenesis: a review of molecular mechanisms, 95 (2014) 495-505.

[13] C. Feng, M. Yang, M. Lan, C. Liu, Y. Zhang, B. Huang, H. Liu, Y.J.O.m. Zhou, c. longevity, ROS: crucial intermediators in the pathogenesis of intervertebral disc degeneration, 2017 (2017).

[14] T. Fulop, J.M. Witkowski, F. Olivieri, A. Larbi, The integration of inflammaging in age-related diseases, Seminars in immunology, Elsevier, 2018, pp. 17-35.

[15] F.J.O. Berenbaum, cartilage, Osteoarthritis as an inflammatory disease (osteoarthritis is not osteoarthrosis!), 21 (2013) 16-21.

[16] S.M. Grundy, H.B. Brewer Jr, J.I. Cleeman, S.C. Smith Jr, C.J.C. Lenfant, Definition of metabolic syndrome: report of the National Heart, Lung, and Blood Institute/American Heart Association conference on scientific issues related to definition, 109 (2004) 433-438.

[17] F. Vasheghani Farahani, The specific in vivo role of PPARgamma and its downstream signaling pathway in the pathophysiology of Osteoarthritis, (2014).

[18] M.J. Armstrong, M.C.J.J.o.l.r. Carey, The hydrophobic-hydrophilic balance of bile salts. Inverse correlation between reverse-phase high performance liquid chromatographic mobilities and micellar cholesterol-solubilizing capacities, 23 (1982) 70-80.

[19] S.R. Rao, S.J.J.J.o.L.R. Fliesler, Cholesterol homeostasis in the vertebrate retina: Biology and pathobiology, (2020) jlr. TR120000979.

[20] T. Nury, A. Zarrouk, A. Vejux, M. Doria, J.M. Riedinger, R. Delage-Mourroux, G.J.B. Lizard, b.r. communications, Induction of oxiapoptophagy, a mixed mode of cell death associated with oxidative stress, apoptosis and autophagy, on 7-ketocholesterol-treated 158N murine oligodendrocytes: Impairment by α-tocopherol, 446 (2014) 714-719.

[21] T. Nury, A. Zarrouk, A. Yammine, J.J. Mackrill, A. Vejux, G.J.B.J.o.P. Lizard, Oxiapoptophagy: A type of cell death induced by some oxysterols, (2020).

[22] J.-S. You, H. Lim, T.-H. Kim, J.-S. Oh, G.-J. Lee, Y.-S. Seo, K. DO KYUNG, S.-K. Yu, H.-J. Kim, C.S.J.A.R. Kim, 25-Hydroxycholesterol Induces Death Receptor-mediated Extrinsic and Mitochondria-dependent Intrinsic Apoptosis in Head and Neck Squamous Cell Carcinoma Cells, 40 (2020) 779-788.

[23] J. Zhao, J. Chen, M. Li, M. Chen, C.J.V. Sun, Multifaceted functions of CH25H and 25HC to modulate the lipid metabolism, immune responses, and broadly antiviral activities, 12 (2020) 727.

[24] W.J. Griffiths, Y.J.T.T.i.A.C. Wang, Sterolomics in biology, biochemistry, medicine, 120 (2019) 115280.

[25] Y.-S. Seo, I.-A. Cho, T.-H. Kim, J.-S. You, J.-S. Oh, G.-J. Lee, D.K. Kim, J.-S.J.T.K.j.o.p. Kim, p.o.j.o.t.K.P. Society, t.K.S.o. Pharmacology, Oxysterol 25-hydroxycholesterol as a metabolic pathophysiological factors of osteoarthritis induces apoptosis in primary rat chondrocytes, 24 (2020) 249.

[26] T.J.B. Yoshimori, b.r. communications, Autophagy: a regulated bulk degradation process inside cells, 313 (2004) 453-458.

[27] J.A. Martin, J.A.J.B. Buckwalter, Aging, articular cartilage chondrocyte senescence and osteoarthritis, 3 (2002) 257-264.

[28] S.V. Garstang, T.P.J.A.j.o.p.m. Stitik, rehabilitation, Osteoarthritis: epidemiology, risk factors, and pathophysiology, 85 (2006) S2-S11.

[29] W. Zhang, M. Doherty, B. Leeb, L. Alekseeva, N. Arden, J. Bijlsma, F. Dinçer, K. Dziedzic, H. Häuselmann, G.J.A.o.t.r.d. Herrero-Beaumont, EULAR evidence based recommendations for the management of hand osteoarthritis: report of a Task Force of the EULAR Standing Committee for International Clinical Studies Including Therapeutics (ESCISIT), 66 (2007) 377-388.

[30] E.P. Kirk, S.J.T.J.o.C.H. Klein, Pathogenesis and pathophysiology of the cardiometabolic syndrome, 11 (2009) 761-765.

[31] A. Courties, J. Sellam, F.J.C.o.i.r. Berenbaum, Metabolic syndrome-associated osteoarthritis, 29 (2017) 214-222.

[32] K. Huffman, W.J.O. Kraus, Cartilage, Osteoarthritis and the metabolic syndrome: more evidence that the etiology of OA is different in men and women, 20 (2012) 603-604.

[33] R. Divella, R. De Luca, I. Abbate, E. Naglieri, A.J.J.o.C. Daniele, Obesity and cancer: the role of adipose tissue and adipo-cytokines-induced chronic inflammation, 7 (2016) 2346.

[34] X. Houard, M.B. Goldring, F.J.C.r.r. Berenbaum, Homeostatic mechanisms in articular cartilage and role of inflammation in osteoarthritis, 15 (2013) 375.

[35] V. Mutemberezi, O. Guillemot-Legris, G.G.J.P.i.l.r. Muccioli, Oxysterols: from cholesterol metabolites to key mediators, 64 (2016) 152-169.

[36] A. Kloudova, F.P. Guengerich, P.J.T.i.E. Soucek, Metabolism, The role of oxysterols in human cancer, 28 (2017) 485-496.

[37] I.J. Martins, Diabetes and cholesterol dyshomeostasis involve abnormal α -synuclein and amyloid beta transport in neurodegenerative diseases, (2015).

[38] E. Olivier, M. Dutot, A. Regazzetti, O. Laprévote, P.J.C. Rat, P.o. Lipids, 25-Hydroxycholesterol induces both P2X7-dependent pyroptosis and caspase-dependent apoptosis in human skin model: New insights into degenerative pathways, 207 (2017) 171-178.

[39] S. Perales, M.J. Alejandre, R. Palomino-Morales, C. Torres, J. Iglesias, A.J.J.o.b. Linares, biotechnology, Effect of oxysterol-induced apoptosis of vascular smooth muscle cells on experimental hypercholesterolemia, 2009 (2009).

[40] A. Trousson, S. Bernard, P.X. Petit, P. Liere, A. Pianos, K. El Hadri, J.M.A. Lobaccaro, M. Said Ghandour, M. Raymondjean, M.J.J.o.n. Schumacher, 25-hydroxycholesterol provokes oligodendrocyte cell line apoptosis and stimulates the secreted phospholipase A2 type IIA via LXR beta and PXR, 109 (2009) 945-958.

[41] Y. Choi, Y. Kim, I. Choi, S.-W. Kim, W.-K.J.F.r.r. Kim, 25-Hydroxycholesterol induces mitochondria-dependent apoptosis via activation of glycogen synthase kinase-3 β in PC12 cells, 42 (2008) 544-553.

[42] C. Travert, S. Carreau, D.J.R.t. Le Goff, Induction of apoptosis by 25-hydroxycholesterol in adult rat Leydig cells: Protective effect of 17β-estradiol, 22 (2006) 564-570.

[43] W.-S. Choi, G. Lee, W.-H. Song, J.-T. Koh, J. Yang, J.-S. Kwak, H.-E. Kim, S.K. Kim, Y.-O. Son, H.J.N. Nam, The CH25H–CYP7B1–RORα axis of cholesterol metabolism regulates osteoarthritis, 566 (2019) 254-258.

[44] J. Buckwalter, H.J.J.o.b. Mankin, j. surgery, Articular cartilage: part ii, 79 (1997) 612.

[45] L. Xu, H. Peng, D. Wu, K. Hu, M.B. Goldring, B.R. Olsen, Y.J.J.o.B.C. Li, Activation of the discoidin domain receptor 2 induces expression of matrix metalloproteinase 13 associated with osteoarthritis in mice, 280 (2005) 548-555.

[46] T. Ichikawa, H. Sugiura, A. Koarai, T. Kikuchi, M. Hiramatsu, H. Kawabata, K. Akamatsu, T. Hirano, M. Nakanishi, K. Matsunaga, 25-Hydroxycholesterol promotes fibroblast-mediated tissue remodeling through NF-jB dependent pathway.

[47] M.B. Goldring, M.J.C.o.i.r. Otero, Inflammation in osteoarthritis, 23 (2011) 471.

[48] S.M. Pokharel, N.K. Shil, Z.T. Colburn, S.-Y. Tsai, J.A. Segovia, T.-H. Chang, S. Bandyopadhyay, S. Natesan, J.C. Jones, S.J.N.c. Bose, Integrin activation by the lipid molecule 25-hydroxycholesterol induces a proinflammatory response, 10 (2019) 1-17.

[49] J. Jang, S. Park, H.J. Hur, H.-J. Cho, I. Hwang, Y.P. Kang, I. Im, H. Lee, E. Lee, W.J.N.c. Yang, 25-hydroxycholesterol contributes to cerebral inflammation of X-linked adrenoleukodystrophy through activation of the NLRP3 inflammasome, 7 (2016) 1-11.

[50] K.L. King, J.A.J.J.o.c.b. Cidlowski, Cell cycle and apoptosis: common pathways to life and death, 58 (1995) 175-180.

[51] H.S. Hwang, H.A.J.I.j.o.m.s. Kim, Chondrocyte apoptosis in the pathogenesis of osteoarthritis, 16 (2015) 26035-26054.

[52] W. Huang, C. Cheng, W.S. Shan, Z.F. Ding, F.E. Liu, W. Lu, W. He, J.G. Xu, Z.S.J.T.F.J. Yin, Knockdown of SGK1 alleviates the IL-1β-induced chondrocyte anabolic and catabolic imbalance by activating FoxO1-mediated autophagy in human chondrocytes, 287 (2020) 94-107.

[53] G. Marino, C.J.C. López-Otín, M.L.S. CMLS, Autophagy: molecular mechanisms, physiological functions and relevance in human pathology, 61 (2004) 1439-1454.

[54] D.J.J.N.r.M.c.b. Klionsky, Autophagy: from phenomenology to molecular understanding in less than a decade, 8 (2007) 931-937.

[55] A. Kihara, Y. Kabeya, Y. Ohsumi, T.J.E.r. Yoshimori, Beclin–phosphatidylinositol 3-kinase complex functions at the trans-Golgi network, 2 (2001) 330-335.

[56] S.-M. Moon, S.A. Lee, S.H. Han, B.-R. Park, M.S. Choi, J.-S. Kim, S.-G. Kim, H.-J. Kim, H.S. Chun, D.K.J.B. Kim, Pharmacotherapy, Aqueous extract of Codium fragile alleviates osteoarthritis through the MAPK/NF-κB pathways in IL-1β-induced rat primary chondrocytes and a rat osteoarthritis model, 97 (2018) 264-270.

ABSTRACT IN KOREAN

7α,25-Dihydroxycholesterol의 자가포식 세포사멸 유도에 의한 병태생리학적 연골퇴행성 분석

김 태 현
조선대학교 대학원 치의생명공학과
(지도교수 : 김 재 성)

콜레스테롤로부터 합성되는 옥시스테롤중의 하나인 25-hydroxycholesterol(25-HC)은 다양한 유형의 세포에서 세포사멸 유도와 관련되어 있으며, 7α,25-dihydroxycholesterol (7α,25-DHC)은 CYP7B1에 의해 합성되는 25-HC의 하위 옥시스테롤이다. 본 연구에서는 연골세포에서 대사 증후군과 관절염 사이의 병태생리학적 이화작용 매개체로서 7α,25-DHC의 자가포식 세포사멸(oxiapoptophagy) 유도에 의한 연골퇴행성을 분석하였다.

본 연구에서 7α,25-DHC의 자가포식 세포사멸 유도에 의한 연골퇴행성 분석을 위해, 흰쥐 연골세포에서 qPCR분석, qRT-PCR 분석, western blot 분석, gelatin zymography 분석, NO 생성 분석, PGE_2 생성 분석, MTT 분석, Hematoxylin & Eosin 분석, 세포 Live & Dead 분석, DAPI 분석, FACS 분석, 면역조직화학 분석, caspase-3/7 활성 분석, 흰쥐 관절연골조직에서 조직학적 분석 및 관절염 동물모델 분석 등을 시행하였다.

7α,25-DHC은 흰쥐 연골세포에서 nitrite와 PGE_2의 생성을 농도 의존적으로 증가시켰으며, 관절연골 구성물질인 aggrecan과 Col II의 mRNA 발현은 농도 의존적으로 감소시켰다. 또한 7α,25-DHC은 MMP-3, MMP-13, iNOS, COX-2 및 PTGS의 mRNA와 단백질의 발현을 농도 의존적으로 증가시켰으며, 이러한 결과는 7α,25-DHC에 의한 연골세포의 염증유도를 시사한다. 7α,25-DHC은 연골세포의 사

멸을 농도 의존적으로 증가시켰으며. apoptosis 소체형성과 핵 응축 현상 등 apoptosis의 전형적인 특성을 유도하였다. 7α,25-DHC은 연골세포에서 세포사멸 유도인자인 FasL의 발현을 농도 의존적으로 증가시키고 이의 하위 세포사멸 인자인 caspase-8을 활성화시켰으며, 이러한 결과는 7α,25-DHC에 의한 연골세포의 외인성 세포사멸(death receptor-mediated extrinsic apoptosis)을 시사한다. 뿐만 아니라 7α,25-DHC은 세포사멸 인자 tBid 활성을 통해 Bax와 Bad 등의 발현을 증가시키고, 세포사멸 억제인자인 Bcl-2와 Bcl-xL의 발현감소를 통해 cytochrom c의 세포질 분비 및 caspase-9를 활성화시켰으며, 이러한 결과는 7α,25-DHC에 의한 연골세포의 미토콘드리아 의존 내인성 세포사멸(mitochondria-mediated intrinsic apoptosis)을 시사한다. 또한 7α,25-DHC에 의해 활성화된 각각의 외인성 및 내인성 세포사멸 인자인 caspase-8과 caspase-9에 의한 caspase-3과 poly ADP-ribose polymerase(PARP)의 활성을 확인하였다. 특히, 7α,25-DHC은 자가포식 바이오마커인 Beclin-1, LC3-I 및 LC3-II의 발현을 증가시켰다. 체외 기관배양 실험에서 7α,25-DHC은 관절연골조직의 caspase-3 발현을 농도 의존적으로 증가시켰다. 뿐만 아니라 7α,25-DHC은 퇴행성관절염 동물모델의 무릎 관절에서 proteoglycan의 발현을 관절연골 퇴행정도에 따라 감소시켰으며, caspase-3와 beclin-1의 발현은 관절연골 퇴행 의존적으로 증가시켰다.

이러한 연구결과는 7α,25-DHC가 연골세포에서 염증을 유도할 뿐만 아니라, 내인성 및 외인성 세포사멸 경로와 더불어 자가포식 기전을 통해 연골세포 사멸을 유도하여 관절연골 퇴행성을 증가시킬 수 있음을 시사한다. 또한 본 연구의 결과는 옥시스테롤 25-HC의 하위 옥시스테롤인 7α,25-DHC가 관절연골 퇴행성과 밀접하게 관련되어 있으며, 대사성 질환과 관절염 사이의 연관성을 제시할 수 있는 병태생리학적 이화작용 매개체임을 제시한다.

감사의 글

이 논문이 완성 될 수 있도록 도와주신 주위의 모든 분들에게 감사의 말씀을 전합니다. 석사 학위 동안 이끌어 주시고 많은 가르침을 지도해주시며 다양한 기회와 끊임없는 격려, 조언 해주신 존경하는 지도 교수님 김재성 교수님께 진심으로 감사드립니다. 또한 항상 응원해주신 김홍중 교수님께 감사드립니다. 그리고 언제나 곁에서 아버지 같은 애정으로 지도해주시며 부족한 저에게 사랑으로 가르침을 주셨던 김도경 교수님 정말 감사드립니다.

광주에서 만나 친동생처럼 챙겨주며, 항상 의지가 되었고 힘들 때 마다 옆에서 다독여 주며 옆에 있으면 항상 즐겁게 되는 형님 강경록, 처음 실험실에 들어와서부터 항상 챙겨주시고 도와주신 영원한 사수 조인아 박사님, 친누나처럼 편했던 이경현 박사님, 대학원 연구실 함께 했던 임향이, 학과 선배이며 누나로써 항상 돌봐주며 챙겨주고 좋아해주신 이슬아 박사님, 시간은 짧지만 내 후배로 들어와서 고생한 차세대 기대주 서정연, 실험에 도움을 주신 문성민 박사님, 그리고 오랫동안 함께한 연구실의 모든 선생님들께 감사드립니다.

나의 영원한 친구이자 가족인 누나 김가은과 누나를 돌봐줘서 항상 고마운 매형 정규호 그리고 귀여운 꿀벌이 조카 정윤서, 광주에서 처음 사귄 친구이며 나를 항상 응원해주는 고마운 이승규, 고향에서 격려해준 김민호, 김광중, 전영배, 박찬영에게 감사드립니다.

마지막으로 오늘에 이르기까지 사랑과 희생으로 돌봐주시고 힘들어할 때 마다 다독여주신 아버지 김진호님, 어머니 양민자 여사님. 항상 아들을 이끌어주시고 지켜봐 주셔서 감사합니다. 더욱 열심히 하여 日新又日新 할 것을 다짐하며 사랑하는 부모님께 논문을 바칩니다.

2020년 12월 논문 편집을 마치며

金 泰 賢